Received: 18 September 2017 | Revised: 29 November 2017 | Accepted: 5 December 2017

DOI: 10.1002/cmr.a.21414

RESEARCH ARTICLE

WILEY

Introduction to average Hamiltonian theory. I. Basics

Andreas Brinkmann

Measurement Science and Standards, National Research Council Canada, Ottawa, ON, Canada

Correspondence
Andreas Brinkmann, Measurement Science and Standards, National Research Council Canada, Ottawa, ON, Canada.
Email: andreas.brinkmann@nrc-cnrc.gc.ca

This article is a contribution to the special issue in honor of Alex Bain.

Abstract

Understanding the dynamics of electron or nuclear spins during a magnetic resonance experiment requires to solve the Schrödinger equation for the spin system considering all contributions to the Hamiltonian from interactions of the spins with each other and their surroundings. In general, this is a difficult task as these interaction terms can be both time-dependent and might not commute with each other. A powerful tool to analytically approximate the time evolution is average Hamiltonian theory, in which a time-independent effective Hamiltonian is taking the place of the time-dependent Hamiltonian. The effective Hamiltonian is subjected to the Magnus expansion, allowing to calculate the effective Hamiltonian to a certain order. The goal of this paper is to introduce average Hamiltonian theory in a rigorous but educational manner. The application to two composite pulses in NMR spectroscopy is used to demonstrate important aspects of average Hamiltonian theory.

KEYWORDS

average Hamiltonian, average Hamiltonian theory, composite pulse, effective Hamiltonian, Magnus expansion

1 | INTRODUCTION

The dynamics of electron and nuclear spins is utilized in the wide area of magnetic resonance-based techniques, including spectroscopy, imaging and microscopy, such as electron paramagnetic resonance (EPR),[1] nuclear magnetic resonance (NMR),[2,3] nuclear quadrupole resonance (NQR)[4] spectroscopy, magnetic resonance imaging (MRI)[5], and magnetic resonance force microscopy (MRFM).[6] However, the dynamics of the electron and nuclear spins is governed by their complex interactions with other spins and with their surroundings, including external magnetic fields, both static and oscillating. Furthermore, predicting the dynamics in most but the simplest cases, requires the use of quantum mechanics, specifically solving the Schrödinger equation for the spin system considering all the contributions of the internal and external interactions to the Hamiltonian. This can be a difficult task especially if the Hamiltonian is time-dependent and the spin interaction terms do not commute, a case in which one needs to either resort to numerical simulations or analytically approximate the spin dynamics to a certain degree or order. The goal of this educational paper is to introduce in a comprehensive and rigorous manner one such powerful analytical approach, *average Hamiltonian theory*,[2,7-10] in which the time-dependent Hamiltonian of the spin system is replaced with a time-independent effective Hamiltonian over a certain time interval, which on its part can be analytically approximated through a series expansion, called Magnus expansion[11] to a certain order in the original Hamiltonian. The beauty of average Hamiltonian theory is that if truncated at any order of the Magnus expansion we are left with a "regular", ie, Hermitian, Hamiltonian that can readily provide physical insight into the underlying spin dynamics.

The time dependence of the spin Hamiltonian stems from two sources: Firstly, the internal spin interactions are modulated by the motions of the molecules holding the spin systems. These motions can be stochastic as the tumbling of the molecules in solution or deterministic as the rotation of the sample in a magic-angle spinning solid-state

NMR experiment. Secondly, nuclear and electron spins may be manipulated effectively by pulses of external oscillating magnetic fields, referred to as radio-frequency (rf) or microwave pulses in case of nuclear and electron spins, respectively. Especially in case of NMR, we are fortunate that the applied rf pulses are able to largely dominate the internal spin interactions, a situation unique compared to other types of spectroscopy. This has enabled the development of an enormous amount of rf pulse sequences not only to directly excite single and multiple quantum coherences, perform spin echoes and achieve population inversion,[12-14] but also to selectively average or *decouple* certain spin interactions during parts of the NMR experiment.[2,8,10,12-14] In magic-angle-spinning solid-state NMR, the averaging of the internal spin interactions by the sample rotation may be suspended over limited time intervals by applying rf pulse sequences that are synchronized with the rotation of the sample. These rf schemes are said to *recouple* certain spin interactions. An almost countless number of such *decoupling* and *recoupling* pulse sequences have been designed during the last 50 years for the application in solution and solid-state NMR spectroscopy often with the crucial help of average Hamiltonian theory.[13,15-17]

This paper is based on educational lectures on average Hamiltonian theory presented at different NMR conferences and solid-state NMR summerschools. It starts with recapitulating some fundamentals of quantum mechanics in Section 2, before introducing average Hamiltonian theory in a general, comprehensive and rigorous manner in Section 3. Finally, part I of this "Introduction to Average Hamiltonian Theory" finishes with the application of average Hamiltonian theory to analytically analyze two composite pulses in Section 4.

2 | FUNDAMENTALS OF QUANTUM MECHANICS

2.1 | Hamiltonian and Schrödiger equation

In quantum mechanics, the state of a physical system at a time point t is represented by its state vector $|\psi(t)\rangle$ in a complex vector space known as Hilbert space or state space.[18-20] Every measurable physical quantity (observable) is described by a Hermitian operator in the state space. The only possible result of the measurement of a physical quantity is one of the eigenvalues (real numbers) of the corresponding Hermitian operator. The time evolution of the quantum state $|\psi(t)\rangle$ is governed by the time-dependent Schrödinger equation

$$\frac{\mathrm{d}}{\mathrm{d}t}|\psi(t)\rangle = -\mathrm{i}H(t)|\psi(t)\rangle, \tag{1}$$

where $H(t)$ is the Hermitian operator, called the *Hamiltonian*, associated with the total energy of the system, here expressed as an angular frequency, ie, the eigenvalues of $H(t)$ multiplied by Planck's constant $\hbar$ give the energy levels in Joules (J). As a consequence, in the following, the eigenvalues of all spin angular momentum operators I_x, I_y, and I_z will be dimensionless.

During an NMR experiment, the macroscopic sample is, in principle, described by a state function, which includes the information about all the electrons and nuclei in the sample. In practice, the time scale of the electron dynamics is usually much shorter than that of the nuclear spin dynamics, which might therefore be described by a state function for the nuclear spin system and a Hamiltonian which only includes terms dependent upon the nuclear spins. This is called the *spin Hamiltonian hypothesis*.[3] In general, nuclear spins interact with magnetic and electric fields stemming from within the sample or from external sources. The contributions to the nuclear spin Hamiltonian relevant for NMR experiments are in detail presented in Refs., 21-24 including the interaction with the external static and oscillating rf fields, and internal spin interactions, such as the chemical shift, quadrupolar coupling, direct dipole coupling, and J-coupling.

2.2 | Time evolution and propagators

If the initial state $|\psi(t_a)\rangle$ of a spin system at time point t_a is known, the state $|\psi(t_b)\rangle$ at a later time point $t_b \geq t_a$ with $T = t_b - t_a$ is determined by solving the Schrödinger equation (Equation 1). The *propagator* or *evolution operator* $U(t_b, t_a)$ is defined as the unitary operator which transforms the spin state $|\psi(t_a)\rangle$ into the spin state $|\psi(t_b)\rangle$:

$$|\psi(t_b)\rangle = U(t_b, t_a)|\psi(t_a)\rangle, \tag{2}$$

where

$$U^{-1}(t_b, t_a) = U^{\dagger}(t_b, t_a) = U(t_a, t_b), \tag{3}$$

The propagation in time is depicted in Figure 1. It is important to note that as a consequence of Equation 2 propagators accumulate from right to left for subsequent time intervals. Take a time point t_c with $t_a \leq t_c \leq t_b$, it then follows

$$U(t_b, t_a) = U(t_b, t_c)U(t_c, t_a). \tag{4}$$

The propagator $U(t, t_a)$ solves the differential equation

$$\begin{aligned} \frac{\mathrm{d}}{\mathrm{d}t}U(t, t_a) &= -\mathrm{i}H(t)U(t, t_a) \\ U(t_a, t_a) &= 1, \end{aligned} \tag{5}$$

which may be obtained by substituting Equation 2 into the Schrödinger equation. Equation 5 is also referred to as the Schrödinger equation for the propagator $U(t, t_a)$. It may also be written as an integral equation that takes the form:

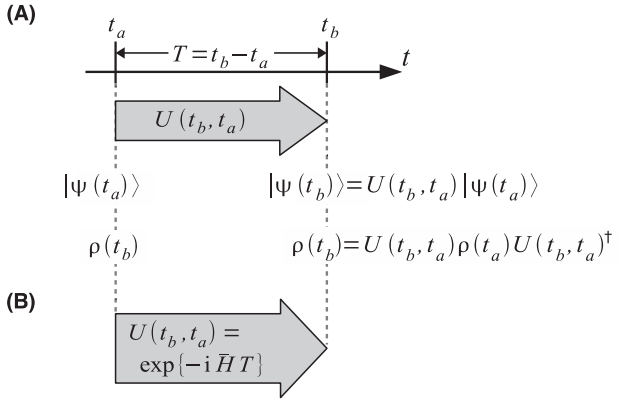

FIGURE 1 Evolution over the time interval $[t_a, t_b]$: A, The propagator $U(t_b, t_a)$ is defined as unitary operator that transforms the spin state $|\psi(t_a)\rangle$ and the density matrix $\rho(t_a)$ at time point t_a into the spin state $|\psi(t_b)\rangle$ and the density matrix $\rho(t_b)$ at time point t_b. B, The time-independent effective Hamiltonian $\bar{H}$ is defined such that $U(t_b, t_a) = \exp\{-i\bar{H}T\}$

$$U(t, t_a) = 1 - \mathrm{i}\int_{t_a}^{t} \mathrm{d}t\, H(t)U(t, t_a). \tag{6}$$

Figure 2 shows schematically the different cases that have to be considered when solving Equation 5 to determine the propagator $U(t_b, t_a)$ over the time interval $[t_a, t_b]$. They are discussed in the following:

i H is time-independent:
Equation (5) can easily be integrated and the propagator be obtained:

$$U(t_b, t_a) = \exp\{-\mathrm{i}HT\}. \tag{7}$$

ii $[H(t'), H(t'')] = 0$ for all time points $t_a \le t', t'' \le t_b$:
The Hamiltonian commutes at all time points in the interval $[t_a, t_b]$. This case is called *inhomogeneous* in the sense of Maricq and Waugh.[25] The propagator can also be derived for this case:

$$U(t_b, t_a) = \exp\left\{-\mathrm{i}\int_{t_a}^{t_b} \mathrm{d}t' H(t')\right\}. \tag{8}$$

iii $[H(t'), H(t'')] \neq 0$ for at least one pair of time points $t_a \le t', t'' \le t_b$:
The Hamiltonian *does not* commute at all time points in the interval $[t_a, t_b]$. This case is called *homogeneous* in the sense of Maricq and Waugh.[25] The propagator cannot, in general, be derived analytically in this case. An *approximate* solution can, however, be determined by different approaches:

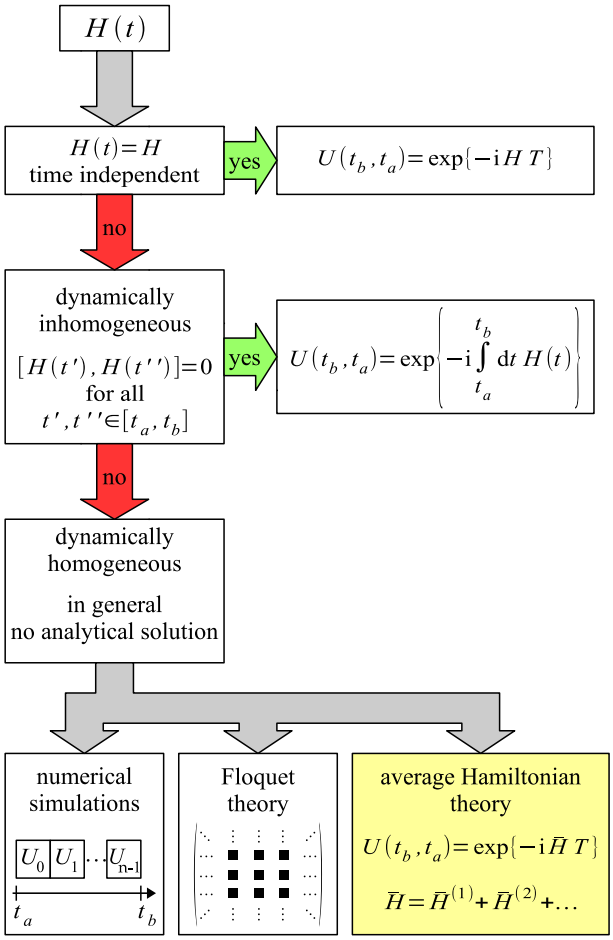

FIGURE 2 Flowchart of the different cases that can be encountered when trying to solve the differential equation (Equation 5) to determine the propagator $U(t_b, t_a)$ over the time interval $[t_a, t_b]$

(a) In numerical simulations, the time interval $[t_a, t_b]$ is divided into a large number of small intervals during which $H(t)$ is considered piecewise time-independent. Consider a division of $[t_a, t_b]$ into n small intervals of length τ_k with $k = 0, 1, \ldots, n - 1$. The propagator in this case is given by

$$U(t_b, t_a) = \exp\{-\mathrm{i}H_{n-1}\tau_{n-1}\}\ldots \exp\{-\mathrm{i}H_k\tau_k\}\ldots\exp\{-\mathrm{i}H_0\tau_0\}, \tag{9}$$

where H_k denotes the time-independent Hamiltonian operative in the kth time interval. In the case that $H(t)$ is not piecewise time-independent, Equation 9 can be considered to be a good approximation if n is sufficiently large. Numerical simulations based on this approach have in detail been discussed by Edén[26-28] in this journal.

(b) In Floquet theory, the time-dependent state-space Hamiltonian $H(t)$ is expanded into a Fourier series.[29,30] The time-independent Fourier components become the elements in a much larger time-

independent Floquet-space Hamiltonian. The expansion of the time-dependent state-space Hamiltonian into the time-independent Floquet-space Hamiltonian is an exact transformation. However, as a result, even in the case of a finite-dimensional state space, the Floquet space becomes infinite-dimensional. Therefore, solving the Schrödinger equation in Floquet space requires to approximate the infinite-dimensional Floquet Hamiltonian with an approximate finite-dimensional Floquet Hamiltonian containing the significant Floquet components. Despite these difficulties, Floquet theory has been used extensively to analyze rf pulse sequences in magic-angle-spinning solid-state NMR.[29,30]

(c) In average, Hamiltonian theory the propagator $U(t_b, t_a)$ is written as an exponential of the form $\exp\{-i\bar{H}T\}$, where $\bar{H}$ is the time-independent and Hermitian *effective* or *average Hamiltonian*. In a following step, $\bar{H}$ may be expanded in a series expansion, called the *Magnus expansion*,[11] where each term in the expansion is Hermitian. One great advantage of the Magnus expansion is that it provides physical insight into the evolution of the quantum system under the propagator $U(t_b, t_a)$. Therefore, average Hamiltonian theory has been very successful in the design of rf pulse sequences both in liquid- and solid-state NMR. In Section 3, average Hamiltonian theory is introduced rigorously. In Section 4, its application to the design and understanding of two composite pulses in NMR is demonstrated.

2.3 | Density operator

Consider an NMR sample containing an ensemble of spin systems, isolated from each other. It is not practical to describe the complete spin-system ensemble by a single state function. Instead, the spin-system ensemble is completely described by the *density operator*

$$\rho(t) = \overline{|\psi_k(t)\rangle\langle\psi_k(t)|} = \sum_k p_k |\psi_k(t)\rangle\langle\psi_k(t)|, \tag{10}$$

where p_k is the probability that an individual spin system is in the spin state $|\psi_k(t)\rangle$.

The time evolution of the density operator $\rho(t)$ is governed by the Liouville-von Neumann equation

$$\frac{\mathrm{d}}{\mathrm{d}t}\rho(t) = -\mathrm{i}[H(t), \rho(t)]. \tag{11}$$

If the initial density operator $\rho(t_a)$ of the spin-ensemble at time point t_a is known, the density operator $\rho(t)$ at a later time point $t \geq t_a$ is obtained by

$$\rho(t) = U(t, t_a)\rho(t)U(t, t_a)^\dagger, \tag{12}$$

where the propagator $U(t, t_a)$ solves Equation 5. Taking the time derivative of Equation 12 and employing the Schrödinger equation (Equation 5) for the propagator result in the Liouville-von Neumann equation (Equation 11), which is therefore equivalent to the Schrödinger equation. It should be noted how the propagator $U(t, t_a)$ "sandwiches" the density operator in Equation 12.

2.4 | Rotation operators and radiofrequency pulses

Nuclear spins may be affected by two different types of rotation in the course of an NMR experiment: (i) spatial rotations, such as the tumbling of molecules in solution or the rotation of the sample as in a magic-angle spinning experiment. (ii) spin rotations caused by rf pulses or spin interactions such as the chemical shift. These two types of rotations are illustrated in Figure 3. It is important to note that these two types of rotations are independent from each other, ie, a rotation of the molecule does not rotate the nuclear spin orientations.

The operators for a rotation of spins I through the angle β about the x-, y-, and z-axis are defined as

$$R_x(\beta) = \exp\{-\mathrm{i}\beta I_x\} \tag{13}$$
$$R_y(\beta) = \exp\{-\mathrm{i}\beta I_y\} \tag{14}$$
$$R_z(\beta) = \exp\{-\mathrm{i}\beta I_z\}. \tag{15}$$

The corresponding rotations are depicted in Figure 4A. As mentioned above, spin rotations can be generated by rf pulses. The Hamiltonian of the interaction of a system of single I-spins with an on-resonance rf field in the high-field approximation and in the rotating frame[3] is given by

$$\begin{aligned} H_{\mathrm{rf}}(t) &= \omega_{\mathrm{nut}}(I_x \cos\phi + I_y \sin\phi) \\ &= \omega_{\mathrm{nut}} R_z(\phi) I_x R_z(-\phi) \end{aligned} \tag{16}$$

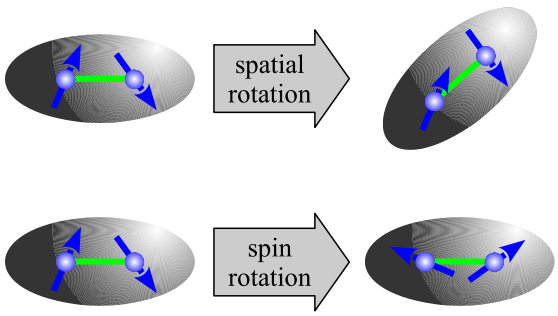

FIGURE 3 Illustration of how spatial and spin rotations affect a two spin-1/2 system represented by blue arrows in a molecule depicted as gray ellipsoid

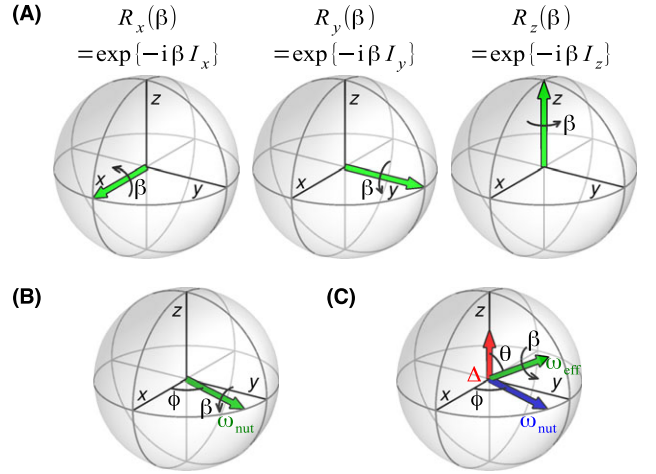

FIGURE 4 A, The rotation operators $R_x(\beta)$, $R_y(\beta)$ and $R_z(\beta)$ produce spin rotations around the *x*-, *y*-, and *z*-axis, respectively. B, An on-resonance rf pulse β_ϕ with nutation frequency ω_{nut} generates a rotation of the nuclear spins by the flip angle β about an axis that lies in the *xy*-plane and encloses the phase angle ϕ with the positive *x*-axis. C, The same rf pulse applied with an rf frequency offset Δ, results in a rotation with the effective field $\omega_{eff} = (\omega_{nut}^2 + \Delta^2)^{1/2}$ about an axis that encloses the angle $\theta = \arctan(\omega_{nut}/\Delta)$ with the positive *z*-axis

where ϕ is the rf phase and ω_{nut} is the nutation frequency of the rf field. In the NMR literature, the symbol ω_1 often is used for the nutation frequency, however here we follow Ref. 3 and use ω_{nut}. If the rf field is applied for a duration τ, the resulting rf pulse, denoted β_ϕ, rotates the nuclear magnetic moments by the *flip angle* β with

$$\beta = \omega_{nut}\tau, \tag{17}$$

about a rotation axis that lies in the *xy*-plane and encloses the *phase* angle ϕ with the positive *x*-axis as shown in Figure 4B. The angles β and ϕ are typically given in degrees when sequences of pulses are specified and given in radians during calculations. Alternatively, we use $\phi = x, y$ if the rotation axis is identical to the positive *x*- or *y*-axis, respectively.

If ω_{nut} and ϕ are time-independent and the rf pulse starts at time point t_a, the propagator during the rf pulse at a time point $t_a \le t \le t_a + \tau$ is given by:

$$U_{rf}(t, t_a) = \exp\{-i\omega_{nut}(t - t_a)(I_x \cos\phi + I_y \sin\phi)\} \tag{18}$$
$$= R_z(\phi)R_x(\omega_{nut}(t - t_a))R_z(-\phi), \tag{19}$$

and the propagator over the complete rf pulse is given by:

$$U_{rf}(t_a + \tau, t_a) = R_z(\phi)R_x(\beta)R_z(-\phi). \tag{20}$$

If the rf field is applied with a frequency offset Δ, the spin Hamiltonian of the interaction with the rf field is given by Equation 16 completed by the resonance offset term:

$$H_{rf}^{\Delta}(t) = \omega_{nut}(I_x \cos\phi + I_y \sin\phi) + \Delta I_z$$
$$= \omega_{nut}R_z(\phi)I_xR_z(-\phi) + \Delta I_z. \tag{21}$$

In order to make this more illustrative, we can define an effective field as shown in Figure 4C with the effective nutation frequency ω_{eff} and the angle θ by which the rotation axis is rotated away from the positive *z*-axis:

$$\omega_{eff} = \sqrt{\omega_{nut}^2 + \Delta^2} \tag{22}$$
$$\theta = \arctan(\omega_{nut}/\Delta). \tag{23}$$

As a result, the Hamiltonian of the rf field in the presence of an rf frequency offset Equation 21 can be written as:

$$H_{rf}^{\Delta}(t) = \omega_{eff}(I_x \sin\theta\cos\phi + I_y \sin\theta\sin\phi + I_z\cos\theta)$$
$$= \omega_{eff}R_z(\phi)R_y(\theta)I_zR_y(-\theta)R_z(-\phi)$$
$$= \omega_{eff}\mathbf{n}\cdot\mathbf{I}, \tag{24}$$

where $\mathbf{n}\cdot\mathbf{I}$ is the scalar product of the normalized polar direction vector $\mathbf{n} = (\sin\theta\cos\phi, \sin\theta\sin\phi, \cos\theta)$ and the spin operator vector $\mathbf{I} = (I_x, I_y, I_z)$.

If ω_{nut}, ϕ and Δ are time-independent and the off-resonance rf pulse with duration τ starts at time point t_a, the propagator during the off-resonance rf pulse at a time point $t_a \le t \le t_a + \tau$ is given by:

$$U_{rf}^{\Delta}(t, t_a) = \exp\{-i\omega_{eff}(t - t_a)\mathbf{n}\cdot\mathbf{I}\}$$
$$= R_z(\phi)R_y(\theta)R_z(\omega_{eff}(t - t_a))R_y(-\theta)R_z(-\phi), \tag{25}$$

and the propagator over the complete off-resonance rf pulse is given by:

$$U_{rf}^{\Delta}(t_a + \tau, t_a) = \exp\{-i\beta_{eff}\mathbf{n}\cdot\mathbf{I}\}$$
$$= R_z(\phi)R_y(\theta)R_z(\beta_{eff})R_y(-\theta)R_z(-\phi), \tag{26}$$

where β_{eff} is the effective flip angle of the pulse around the direction $\mathbf{n}$ of the effective field,

$$\beta_{eff} = \omega_{eff}\tau = \frac{\beta}{\sin\theta} = \frac{\Delta\tau}{\cos\theta}, \tag{27}$$

where the alternative expressions in Equation 27 allow us to easily identify the two limiting cases: (i) $\theta = \pi/2$, resulting in $\beta_{eff} = \beta$, hence for an on-resonance pulse ($\Delta = 0$) the expected flip angle β is obtained. (ii) $\theta = 0$, resulting in $\beta_{eff} = \Delta\tau$, hence for the case where the nutation frequency of the rf field is zero ($\omega_{nut} = 0$), the evolution corresponds to the spin precession by the angle $\Delta\tau$ due to the resonance offset.

3 | AVERAGE HAMILTONIAN THEORY

After being briefly introduced in Section 2.2, here average Hamiltonian theory is presented more rigorously.

3.1 | Effective Hamiltonian and Magnus expansion

Consider again the evolution of the spin system over the time interval $[t_a, t_b]$ with $T = t_b - t_a$ by the propagator $U(t_b, t_a)$ as introduced in Section 2.2 and depicted in Figure 1. The propagator is a solution to Equation 5, governed by the time-dependent Hamiltonian $H(t)$. It is both useful and insightful to define a time-independent *effective* or *average Hamiltonian* $\bar{H}$ through

$$U(t_b, t_a) = \exp\{-i\bar{H}T\}, \tag{28}$$

analog to the case of Equation 7, in which the Hamiltonian H is time-independent over the interval $[t_a, t_b]$.

The effective Hamiltonian may be expanded in a series expansion, called the Magnus expansion:[11]

$$\bar{H} = \bar{H}^{(1)} + \bar{H}^{(2)} + \bar{H}^{(3)} + \bar{H}^{(4)} + \dots \tag{29}$$

where the term $\bar{H}^{(n)}$ is referred to as the nth order average Hamiltonian. If the expansion is terminated at the nth order, the effective Hamiltonian $\bar{H}$ in Equation 29 and the resulting propagator in Equation 28 are said to have been calculated in nth order average Hamiltonian theory. The first four orders of the Magnus expansion are given by

$$\bar{H}^{(1)} = \frac{1}{T}\int_{t_a}^{t_b} \mathrm{d}t\, H(t) \tag{30}$$

$$\bar{H}^{(2)} = \frac{1}{2iT}\int_{t_a}^{t_b} \mathrm{d}t \int_{t_a}^{t} \mathrm{d}t' \left[H(t), H(t')\right] \tag{31}$$

$$\begin{aligned}\bar{H}^{(3)} = -\frac{1}{6T}\int_{t_a}^{t_b} \mathrm{d}t \int_{t_a}^{t} \mathrm{d}t' \int_{t_a}^{t'} \mathrm{d}t'' \Big\{ &\Big[H(t), \left[H(t'), H(t'')\right]\Big] \\ &+ \Big[\left[H(t), H(t')\right], H(t'')\Big]\Big\}\end{aligned} \tag{32}$$

$$\begin{aligned}\bar{H}^{(4)} = -\frac{1}{12iT}\int_{t_a}^{t_b} \mathrm{d}t \int_{t_a}^{t} \mathrm{d}t' \int_{t_a}^{t'} \mathrm{d}t'' \int_{t_a}^{t''} \mathrm{d}t''' \\ \times \Big\{ \Big[\Big[\left[H(t), H(t')\right], H(t'')\Big], H(t''')\Big] \\ + \Big[H(t), \Big[\left[H(t'), H(t'')\right], H(t''')\Big]\Big] \\ + \Big[H(t), \Big[H(t'), \left[H(t''), H(t''')\right]\Big]\Big] \\ + \Big[H(t'), \Big[H(t''), \left[H(t'''), H(t)\right]\Big]\Big]\Big\}\end{aligned} \tag{33}$$

It should be noted that the indexing of the Magnus expansion is equal to the order to which the Hamiltonian $H(t)$ appears in the respective expression. Hence, the indexing starts with one, whereas older literature on average Hamiltonian theory uses indices that are one less than those given here.[7,8] The fourth order expression given above is based on those published by Wilcox,[31] Bialynicki-Birula et al[32] and later by Klarsfeld and Oteo.[33] An important property of the Magnus expansion is that each term $\bar{H}^{(n)}$ in the expansion is Hermitian, resulting also in a Hermitian effective Hamiltonian in any order of truncation. This ensures that the propagator is indeed unitary in any order of average Hamiltonian theory. Furthermore, since the effective Hamiltonian $\bar{H}$ and the propagator $U(t_b, t_a)$ are time-independent, they enable an *illustrative* interpretation of the *average* quantum dynamics under the time-dependent Hamiltonian $H(t)$ during the time interval $[t_a, t_b]$. However, the effective Hamiltonian *does not* allow to predict the *exact* dynamics of the spin system *during* the time interval $[t_a, t_b]$.

The Magnus expansion converges rapidly if, for any time $t_a \le t \le t_b$, the condition

$$\|H(t)\|T \ll 1 \tag{34}$$

is fulfilled, where the norm, $\|H(t)\|$, might, for example, be chosen to be

$$\|H(t)\| = \left(\mathrm{Tr}\{H(t)^2\}\right)^{1/2}. \tag{35}$$

The condition in Equation 34 is very conservative and is not necessary fulfilled in many practical applications of the Magnus expansion.

From Equations 30-33, the following four special cases can be readily identified:

i $[H(t'), H(t'')] = 0$ for all time points $t_a \le t', t'' \le t_b$:
This inhomogeneous case has been discussed before, see Equation 8. As the Hamiltonian commutes at all time points in the interval $[t_a, t_b]$, all average Hamiltonian terms with order higher than one are equal to zero:

$$\bar{H}^{(n)} = 0 \qquad \text{for all } n > 1, \tag{36}$$

and as a result, the exact effective Hamiltonian is given by the first order average Hamiltonian:

$$\bar{H} = \bar{H}^{(1)}. \tag{37}$$

ii $H(t)$ is symmetric:
If $H(t_a + \tau) = H(t_b - \tau)$ for any $0 \le \tau \le (t_b - t_a)$, $H(t)$ is referred to as being *symmetric* in time over the time interval $[t_a, t_b]$. In this case, all even order average Hamiltonian terms are equal to zero, as shown first by Mansfield:[34]

$$\bar{H}^{(n)} = 0 \qquad \text{for all even n,} \tag{38}$$

leading to

$$\bar{H} = \bar{H}^{(1)} + \bar{H}^{(3)} + \bar{H}^{(5)} + \ldots \tag{39}$$

This is an important property and tool in the design of multiple pulse sequences, where often a particular first order average Hamiltonian is desired, whereas higher orders ideally should disappear, especially in the presence of errors in the pulse sequence or large disruptive spin interactions, such as rf frequency offsets or chemical shift anisotropies.[8,34,35]

iii $H(t)$ is antisymmetric:
If $H(t_a + \tau) = -H(t_b - \tau)$ for any $0 \le \tau \le (t_b - t_a)$, $H(t)$ is referred to as being *antisymmetric* in time over the time interval $[t_a, t_b]$. This case results in all orders of average Hamiltonian terms disappearing:[34]

$$\bar{H}^{(n)} = 0 \qquad \text{for all n,} \tag{40}$$

which leads to

$$\bar{H} = 0 \tag{41}$$

$$U(t_b, t_a) = 1, \tag{42}$$

ie, the propagator is identical to unity, hence the spin system at time point t_b has returned to its initial state at time point t_a. Although this might look trivial, NMR techniques exploiting this characteristic, such as spin echoes[36] and rotational echoes[25] are highly important over a wide range of applications.

iv $H(t)$ is piecewise time-independent: The last case we would like to consider in this list is that of a Hamiltonian $H(t)$, which is piecewise time-independent over the interval $[t_a, t_b]$. Consider the division of $[t_a, t_b]$ into N subintervals $[t_k, t_{k+1}]$ with durations $\tau_k = t_{k+1} - t_k$, so that

$$H(t) = H_k \quad \text{for} \quad t_k \le t \le t_{k+1} \quad \text{and} \quad k = 1, \ldots, N, \tag{43}$$

where $t_1 \equiv t_a$ and $t_{N+1} \equiv t_b$. In this case, the first two orders of the Magnus expansion in general are given by

$$\bar{H}^{(1)} = \frac{1}{T}\sum_{k=1}^{N} H_k \tau_k \tag{44}$$

$$\bar{H}^{(2)} = \frac{1}{2iT}\sum_{k=2}^{N}\sum_{l=1}^{k-1}\left[H_k, H_l\right]\tau_k\tau_l. \tag{45}$$

The third order is more complicated to write out in general. Therefore, we consider the simple case of two subintervals of $[t_a, t_b]$ over which $H(t)$ is piecewise time-independent. This is depicted in Figure 5. In this case, the first three orders of the Magnus expansion simplify to

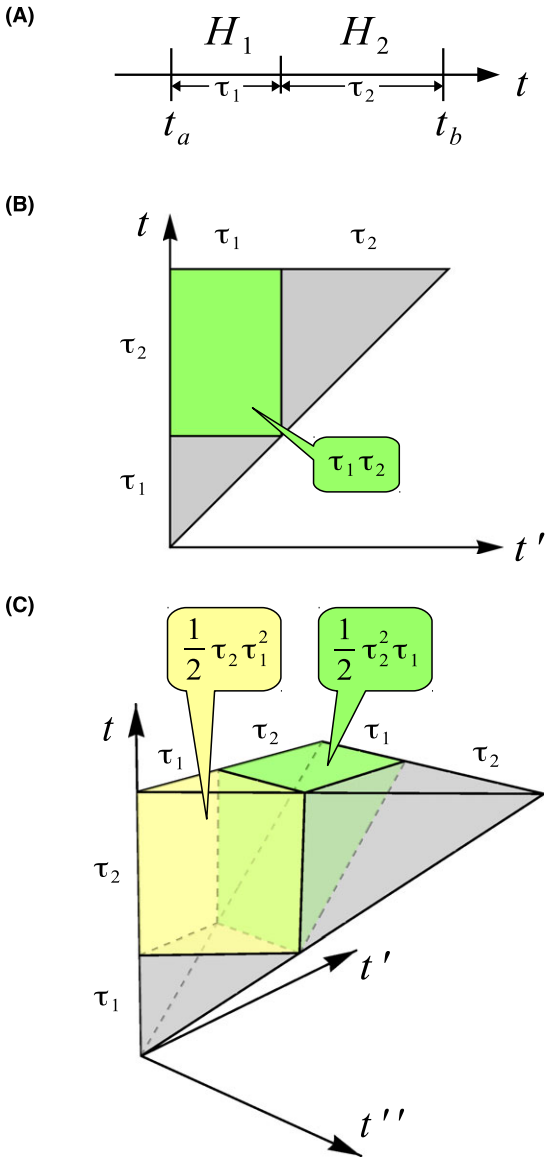

FIGURE 5 Integration intervals, areas and volumes in A, first, B, second, and C, third order average Hamiltonian theory of a Hamiltonian that is piecewise time-independent

$$\bar{H}^{(1)} = \frac{1}{T}\left\{H_1\tau_1 + H_2\tau_2\right\} \tag{46}$$

$$\bar{H}^{(2)} = \frac{1}{2iT}\left[H_2, H_1\right]\tau_2\tau_1 \tag{47}$$

$$\bar{H}^{(3)} = -\frac{1}{12T}\left\{\left[H_2, \left[H_2, H_1\right]\right]\tau_2^2\tau_1 + \left[\left[H_2, H_1\right], H_1\right]\tau_2\tau_1^2\right\}, \tag{48}$$

where the integration intervals, areas and volumes for each order are shown in Figure 5, respectively. Since the Hamiltonian is piecewise time-independent solely, *pairwise different* blocks have to be considered in the commutators in Equations 31 and 32. Hence, solely the integral over the area of size $\tau_2\tau_1$ highlighted in green in

Figure 5B contributes to $\bar{H}^{(2)}$ in Equation 31 resulting in Equation 47. Similarly, solely the integrals over the two volumes of sizes $\tau_2\tau_1^2/2$ and $\tau_2^2\tau_1/2$ shown in yellow and green in Figure 5C, respectively, contribute to $\bar{H}^{(3)}$ in Equation 32 leading to the result in Equation 48.

3.2 | Interaction frame

As discussed in Section 3.1, the Magnus expansion Equation 29 of the effective Hamiltonian over the time interval $[t_a, t_b]$ only converges if the norm of the Hamiltonian $H(t)$ is small, see the convergence condition Equation 34. However, the convergence of the Magnus expansion may be improved drastically by transforming the Hamiltonian $H(t)$ into a suitable *interaction frame*, often referred to as *interaction picture* or *interaction representation* in textbooks on quantum mechanics.[19,20] Consider the case where the Hamiltonian may be expressed as a sum of two terms

$$H(t) = H_A(t) + H_B(t), \tag{49}$$

where both parts may be time-dependent and might not commute in general. Here, $H_A(t)$ is the larger part and should be chosen in such a way that the propagator $U_A(t, t_a)$, solving the equation

$$\frac{\mathrm{d}}{\mathrm{d}t}U_A(t,t_a) = -\mathrm{i}H_A(t)U_A(t,t_a) \tag{50}$$

$$U_A(t_a,t_a) = 1, \tag{51}$$

can easily be determined analytically. It proves to be a useful ansatz to express $U(t, t_a)$ as the product of $U_A(t, t_a)$ and the so-called interaction frame propagator $\tilde{U}(t,t_a)$:

$$U(t,t_a) = U_A(t,t_a)\tilde{U}(t,t_a). \tag{52}$$

Inserting this ansatz into Equation 5 leads to

$$\frac{\mathrm{d}}{\mathrm{d}t}\tilde{U}(t,t_a) = \underbrace{-\mathrm{i}\left(U_A^\dagger(t,t_a)H(t)U_A(t,t_a) - \mathrm{i}U_A^\dagger(t,t_a)\left(\frac{d}{dt}U_A(t,t_a)\right)\right)}_{\tilde{H}(t)}\tilde{U}(t,t_a), \tag{53}$$

where we have defined the interaction frame Hamiltonian $\tilde{H}(t)$ such that the interaction frame propagator $\tilde{U}(t,t_a)$ solves the differential equation

$$\frac{\mathrm{d}}{\mathrm{d}t}\tilde{U}(t,t_a) = -\mathrm{i}\tilde{H}(t)\tilde{U}(t,t_a) \tag{54}$$

$$\tilde{U}(t_a,t_a) = 1. \tag{55}$$

The interaction frame Hamiltonian $\tilde{H}(t)$ defined in Equation 53 may be simplified using Equations 49 and 50 such that one obtains:

$$\tilde{H}(t) = \tilde{H}_B(t) = U_A(t,t_a)^\dagger H_B(t) U_A(t,t_a). \tag{56}$$

Note that the propagator $U_A(t, t_a)$, which depends upon two time points, is used as the transformation operator, which strictly spoken should only depend upon the time point t.[37]

If we consider again the scenario depicted in Figure 1 and described in Section 3.1, ie, the evolution of the spin system over the time interval $[t_a, t_b]$ with $T = t_b - t_a$ under the Hamiltonian shown in Equation 49, the propagator $U(t_b, t_a)$ may therefore be written as:

$$U(t_b,t_a) = U_A(t_b,t_a)\tilde{U}(t_b,t_a), \tag{57}$$

where the interaction frame propagator $\tilde{U}(t_b,t_a)$ may be expressed in terms of an effective interaction frame Hamiltonian $\bar{H}_B$ analogous to Equation 28 and analyzed by the Magnus expansion Equation 29:

$$\tilde{U}(t_b,t_a) = \exp\{-\mathrm{i}\bar{H}_B T\} \tag{58}$$

$$\bar{H}_B = \bar{H}_B^{(1)} + \bar{H}_B^{(2)} + \bar{H}_B^{(3)} + \bar{H}_B^{(4)} + \ldots \tag{59}$$

The individual orders of the Magnus expansion are given by Equations 30-33, where the Hamiltonian $H(t)$ has to be replaced by the interaction frame Hamitlonian $\tilde{H}(t) = \tilde{H}_B(t)$.

In practice, the choice of the interaction frame depends on the particular Hamiltonian relevant to the problem under study. For example, in NMR spectroscopy, the dominating term in the spin Hamiltonian is the Zeeman interaction of the spins with the external static magnetic field. The interaction frame of the Zeeman interaction is referred to as the *rotating frame* and the spin Hamiltonian commonly used in NMR spectroscopy corresponds to the first, and sometimes second, order average Hamiltonian in the rotating frame of the Zeeman interaction.[2,3,9,38,39] Once the NMR Hamiltonian is presented in the rotating frame, other interactions become suitable choices for a further interaction frame transformation.

A common choice in the application of average Hamiltonian theory to the design of rf pulse sequences is to transform the rotating frame spin Hamiltonian into the interaction frame of the rf field, also commonly referred to as the *toggling frame*.[8] Another possible choice is the interaction frame of a dominating *internal* spin interaction in the rotating frame such as the chemical shift anisotropy or the quadrupolar coupling, sometimes referred to as the *jolting frame*.[40] However, rather than using the terms "toggling frame" and "jolting frame", I would for clarity instead recommend using the term "interaction frame of…".

3.3 | Periodic Hamiltonian

Many interactions of the nuclear spins within the spin system and with external magnetic fields are periodic in time, modulated for example by periodic sequences of rf pulses or by the rotation of the sample in magic-angle spinning experiments. In this section, we would like to extend average Hamiltonian theory to the case of periodic spin Hamiltonians $H(t)$:

$$H(t+NT) = H(t). \tag{60}$$

where T is the period of the Hamiltonian and N is any integer. This case is shown schematically in Figure 6. It is particularly useful to choose one period as the interval $[t_a,\ t_b]$ with $T = t_b - t_a$ over which the effective Hamiltonian $\bar{H}$ should be determined according to Equation 28. This enables us to reuse the effective Hamiltonian to propagate the spin system over integer multiplies of T:

$$U(t_a+T,t_a) = U(t_b,t_a) = \exp\{-\mathrm{i}\bar{H}T\} \tag{61}$$
$$U(t_a+NT,t_a) = \exp\{-\mathrm{i}\bar{H}NT\} \tag{62}$$

The effective Hamiltonian $\bar{H}$ over one period T may now be analyzed by the Magnus expansion Equation 29 as described in detail in Section 3.1.

Perhaps more interesting is the case where we would like to transform a periodic Hamiltonian into the interaction frame of a dominant term in the Hamiltonian. Analogous to the case discussed in the previous Section 3.2, the periodic Hamiltonian $H(t)$ is expressed as sum of two terms

$$H(t) = \overbrace{H_A(t)}^{\substack{\text{periodic}\\ H_A(t+NT)=H_A(t)}} + \overbrace{H_B(t)}^{\substack{\text{periodic}\\ H_B(t+NT)=H_B(t)}} \tag{63}$$

where we have indicated that both terms $H_A(t)$ and $H_B(t)$ need to be periodic with the same period T as $H(t)$ itself. This ensures that also the interaction frame Hamiltonian $\tilde{H}(t) = \tilde{H}_B(t)$ in Equation 56 is periodic:

$$\tilde{H}_B(t) = U_A(t,t_a)^{\dagger} H_B(t) U_A(t,t_a) \tag{64}$$
$$\tilde{H}_B(t+NT) = \tilde{H}_B(t) \tag{65}$$

The resulting total propagator over a single period T may be calculated according to Equation 57:

$$\begin{aligned} U(t_a+T,t_a) &= U_A(t_a+T,t_a)\tilde{U}(t_a+T,t_a) \\ &= U_A(t_a+T,t_a)\exp\{-\mathrm{i}\bar{H}_B T\}. \end{aligned} \tag{66}$$

Similar as in Equation 62, we may reuse the effective Hamiltonian to determine the propagator at multiples of T:

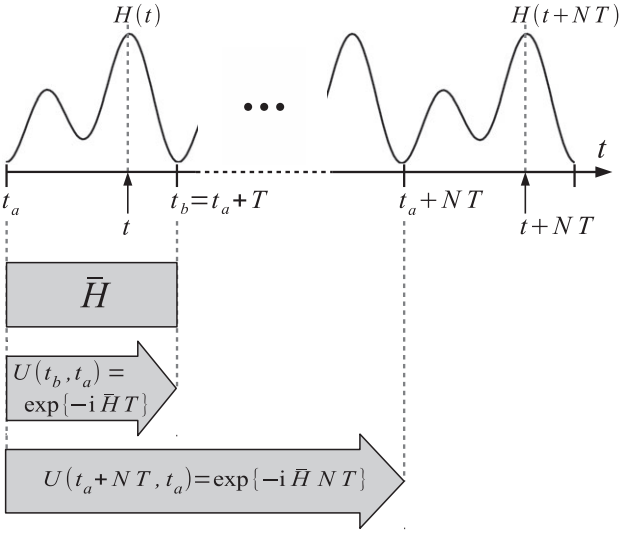

FIGURE 6 Visualization of a Hamiltonian $H(t)$ that is periodic in time with period T. If the effective Hamiltonian $\bar{H}$ is determined over one period T, it is straightforward to obtain the propagator over time intervals that are integer multiples of T

$$U(t_a+NT,t_a) = \left(U_A(t_a+T,t_a)\exp\{-\mathrm{i}\bar{H}_B T\}\right)^N, \tag{67}$$

where we note that $U_A(t_a + T,t_a)$ and $\exp\{-\mathrm{i}\bar{H}_B T\}$ do not necessarily commute, hence this result cannot be further simplified in general.

However, in most of the literature on average Hamiltonian theory, another condition is imposed on $H_A(t)$, namely that it needs to be *cyclic*, ie, its propagator $U_A(t_b, t_a)$ over the period T needs to be positive or negative identity, returning the spins at time point t_b, after the evolution time T, back to its original state they were in at time point t_a:[2,7-10]

$$U_A(t_b,t_a) = \pm 1. \tag{68}$$

In this case, Equations 66 and 67 straightforwardly simplify to

$$U(t_a+T,t_a) = \exp\{-\mathrm{i}\bar{H}_B T\} \tag{69}$$
$$U(t_a+NT,t_a) = \exp\{-\mathrm{i}\bar{H}_B NT\}. \tag{70}$$

3.4 | Average Hamiltonian theory summary sheet

In Sections 3.1-3.3, we have not only introduced average Hamiltonian in general but also considered more advanced topics such as the interaction frame and periodic Hamiltonians. In light of the significant amount of material, the reader had to follow up to this point, Figure 7 provides an overview and summary sheet of average Hamiltonian theory that is covered in this paper, it is presented as a flowchart or decision tree: On the top, we start with the

time-dependent Hamiltonian $H(t)$ of the spin system. Depending on whether the Hamiltonian is periodic in time or not, either the left or right route is taken. In the next step, it is distinguished if the Hamiltonian can be written as the sum of two terms, $H_A(t)$ and $H_B(t)$, so that a transformation into the interaction frame can be performed before the Magnus expansion is applied. Hence, in total, four cases are shown in the overview sheet, where the last two rows show how the Magnus expansion is performed and the propagator appears. The reader is encouraged to consult this overview sheet whenever applying average Hamiltonian theory in practice and to dive back into Sections 3.1-3.3 for details.

4 | COMPOSITE PULSES

After having laid the groundwork of average Hamiltonian theory in the previous sections, it is time to step-by-step work through a couple of examples, for educational purposes in far more detail than is usually encountered in the NMR literature. One prominent area in NMR that benefited from the application of average Hamiltonian theory in the 1980s was the development of so-called *composite pulses*.[12-14] A composite pulse is a series of rectangular rf pulses that replace a single rectangular rf pulse in a pulse sequence. Under ideal conditions, ie, the spin system solely experiences the Zeeman interaction and the interaction with the rf field, the transformation of the spin system imposed by the composite pulse is identical to the one imposed by the rectangular pulse it replaces.[12-14] However, composite pulses are commonly designed such that they are less sensitive to the exact setting of the rf field amplitude and frequency offset. In this section, we will examine in detail two seminal composite 180° pulses by average Hamiltonian theory.

4.1 | The composite pulse 90_y180_x90y

The first composite pulse we will study by average Hamiltonian theory is a group of three pulses $90_y180_x90_y$, which under ideal conditions is equivalent to a 180_x pulse. It was first constructed using geometrical arguments by Levitt and Freeman as an inversion pulse that is compensated with respects to missetting of the rf amplitude.[41] In this section, the consequences of such an rf amplitude error on the transformation of the spin system during the composite pulse will be analyzed by average Hamiltonian theory and compared with exact calculations and the performance of a single rf pulse.

The composite pulse $90_y180_x90_y$ together with its timing is depicted in Figure 8A. The three consecutive pulses are labeled ①, ②, and ③. The starting time point of the sequence is denoted t_0, the time point after the first 90_y pulse ① is labeled t_1, the time point after the 180_x pulse ② is denoted t_2, and the time point after the final 90_y pulse ③ is labeled t_3. Consequently, the durations of the individual pulses and the complete composite pulse are given by $\tau_1 = t_1 - t_0$, $\tau_2 = t_2 - t_1$, $\tau_3 = t_3 - t_2$, and $T = t_3 - t_1 = \tau_1 + \tau_2 + \tau_3$, respectively. The ideal nutation frequency throughout the composite pulse is constant and given by ω_{nut}. Hence, the following relationships are fulfilled for the flip angles and durations of the pulses:

$$\begin{aligned} \omega_{nut}\tau_1 &= \omega_{nut}\tau_3 = \frac{\pi}{2} \\ \omega_{nut}\tau_2 &= \pi \\ \omega_{nut}T &= 2\pi \end{aligned} \tag{71}$$

The *absolute* rf amplitude error is denoted ω_ϵ, hence the total rf amplitude during the composite pulse is given by $\omega_{nut} + \omega_\epsilon$. We can also define a *relative* rf amplitude error ϵ as the ratio $\epsilon = \omega_\epsilon/\omega_{nut}$.

4.1.1 | Hamiltonian

Consider a system of single I-spins that are subject solely to the Zeeman interaction and the interaction with the rf field during the composite pulse shown in Figure 8A. The Hamiltonian at time point t in the high-field approximation and in the rotating reference frame[3] is according to Equation 16 given by

$$\begin{aligned} H(t) &= (\omega_{nut} + \omega_\epsilon)(I_x \cos\phi(t) + I_y \sin\phi(t)) \\ &= (\omega_{nut} + \omega_\epsilon)R_z(\phi(t))I_xR_z(-\phi(t)) \\ &= \underbrace{\omega_{nut}R_z(\phi(t))I_xR_z(-\phi(t))}_{H_A(t)} + \underbrace{\omega_\epsilon R_z(\phi(t))I_xR_z(-\phi(t))}_{H_B(t)}, \end{aligned} \tag{72}$$

where $\phi(t)$ is the rf phase at time point t during the composite pulse. In the last line of Equation 72, the Hamiltonian has been written as the sum of two parts $H_A(t)$ and $H_B(t)$, where $H_A(t)$ corresponds to the Hamiltonian of the interaction with the ideal rf field and $H_B(t)$ is the small perturbation Hamiltonian of the rf amplitude error. Naturally, as outlined in Section 3.2, this offers the opportunity to transform the Hamiltonian $H(t)$ into the interaction frame of $H_A(t)$ before applying average Hamiltonian theory. As a result, since $H(t)$ is non-periodic, this case falls into the second column of Figure 7. For the different time periods during the composite pulse, $H_A(t)$ and $H_B(t)$ are explicitly given by:

$$H_A(t) = \begin{cases} \omega_{nut}I_y & \text{for} \quad t_0 \le t < t_1 \text{ or } t_2 \le t \le t_3 \\ \omega_{nut}I_x & \text{for} \quad t_1 \le t < t_2 \end{cases} \tag{73}$$

and

$$H_B(t) = \begin{cases} \omega_\epsilon I_y & \text{for} \quad t_0 \le t < t_1 \text{ or } t_2 \le t \le t_3 \\ \omega_\epsilon I_x & \text{for} \quad t_1 \le t < t_2. \end{cases} \tag{74}$$

4.1.2 | Rf propagator

In order to transform $H(t)$ in Equation 72 into the interaction frame of $H_A(t)$, we need to calculate the rf propagator

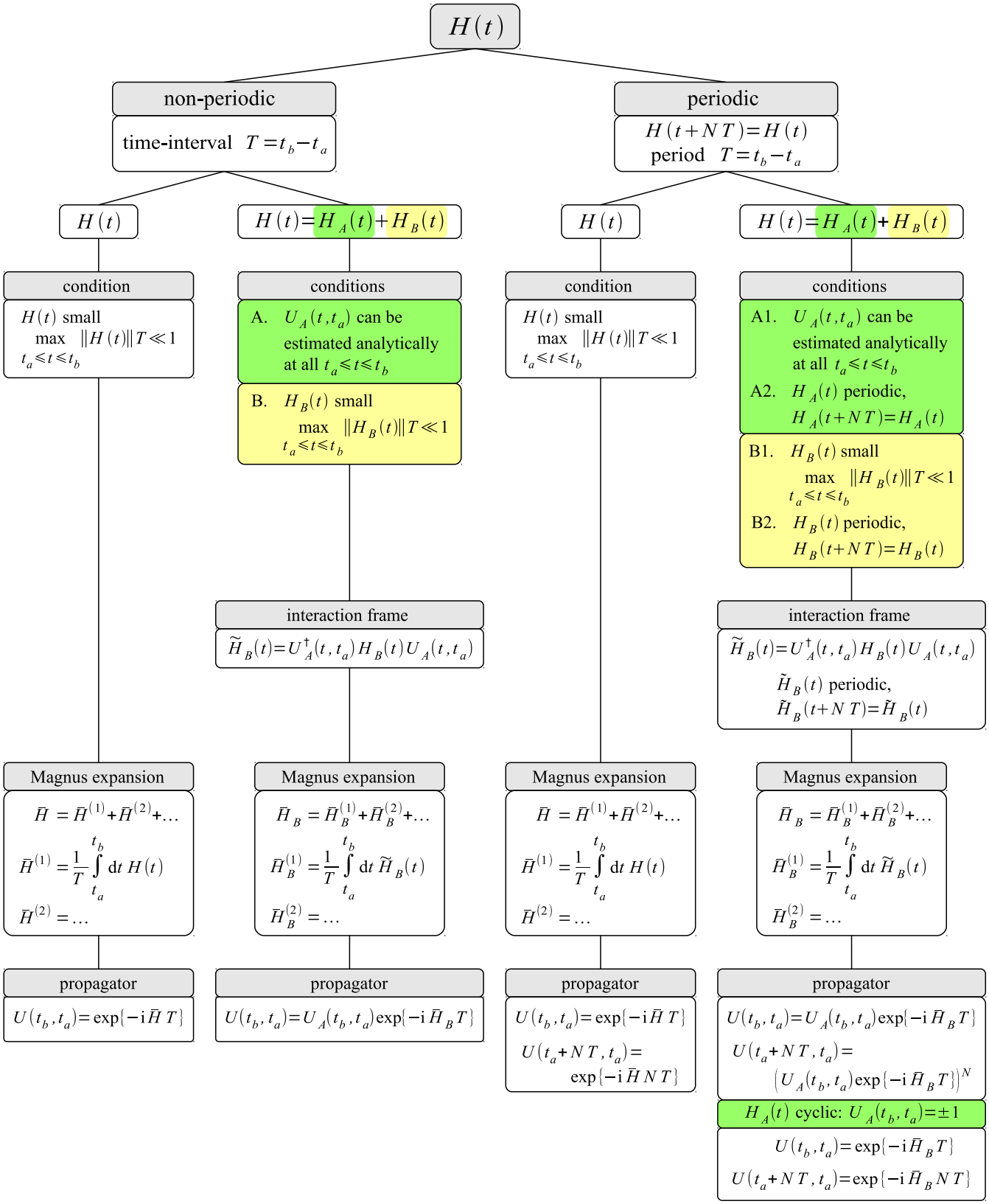

FIGURE 7 Overview and summary sheet of average Hamiltonian theory

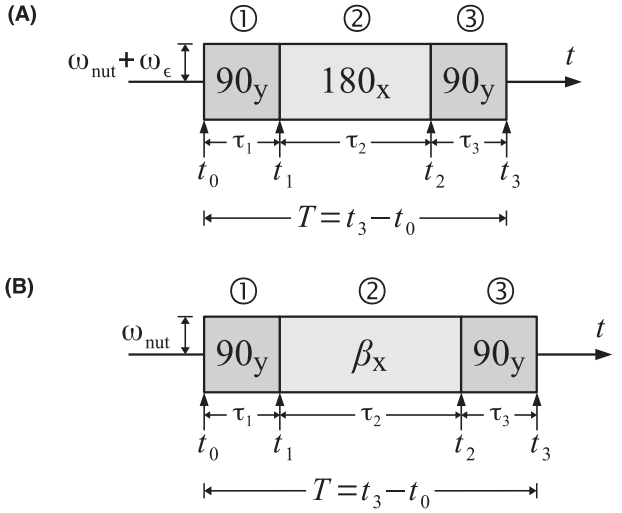

FIGURE 8 Timing Diagrams of the two composite inversion pulses discussed in the text using average Hamiltonian theory: A, the $90_y180_x90_y$ composite pulse, and B, the $90_y\beta_x90_y$ composite pulse, where the flip angle β will be optimized such that the resulting inversion pulse is compensated with respect to rf frequency offsets in first order average Hamiltonian theory

solving the corresponding Schrödinger equation (Equation 50). Since the Hamiltonian is piecewise time-independent during the composite pulse, this is straightforward:

$$U_A(t,t_0) = \begin{cases} R_y(\omega_{\text{nut}}(t-t_0)) & \text{for } t_0 \le t < t_1 \\ R_x(\omega_{\text{nut}}(t-t_1))R_y\left(\frac{\pi}{2}\right) & \text{for } t_1 \le t < t_2 \\ R_y(\omega_{\text{nut}}(t-t_2))R_x(\pi)R_y\left(\frac{\pi}{2}\right) & \text{for } t_2 \le t \le t_3. \end{cases} \tag{75}$$

Note how the propagators accumulate from right to left in the second and third line, see also Equation 4. In the next step, we use the time-dependent flip angles $\beta_{①}(t) = \omega_{\text{nut}}(t-t_0)$, $\beta_{②}(t) = \omega_{\text{nut}}(t-t_1)$ and $\beta_{③}(t) = \omega_{\text{nut}}(t-t_2)$ to simplify the propagator expression:

$$U_A(t,t_0) = \begin{cases} R_y(\beta_{①}(t)) & \text{for } t_0 \le t < t_1 \\ R_x(\beta_{②}(t))R_y\left(\frac{\pi}{2}\right) & \text{for } t_1 \le t < t_2 \\ R_y\left(\beta_{③}(t) - \frac{\pi}{2}\right)R_x(\pi) & \text{for } t_2 \le t \le t_3, \end{cases} \tag{76}$$

where we used in the last line the transformation

$$R_x(\pi)R_y\left(\frac{\pi}{2}\right) = R_x(\pi)R_y\left(\frac{\pi}{2}\right)R_x(-\pi)R_x(\pi) = R_y\left(-\frac{\pi}{2}\right)R_x(\pi). \tag{77}$$

Finally, for the transformation into the interaction frame, we also need to calculate the adjoint of the rf propagator:

$$U_A^{\dagger}(t,t_0) = \begin{cases} R_y(-\beta_{①}(t)) & \text{for } t_0 \le t < t_1 \\ R_y\left(-\frac{\pi}{2}\right)R_x(-\beta_{②}(t)) & \text{for } t_1 \le t < t_2 \\ R_x(-\pi)R_y\left(-\beta_{③}(t) + \frac{\pi}{2}\right) & \text{for } t_2 \le t \le t_3. \end{cases} \tag{78}$$

4.1.3 | Interaction frame Hamiltonian

With the help of the rf propagators calculated in the previous section, we can now transform the Hamiltonian $H(t)$ into the interaction frame of $H_A(t)$ as shown in Equation 56:

$$\tilde{H}_B(t) = \begin{cases} R_y(-\beta_{①}(t))\omega_\epsilon I_y R_y(\beta_{①}(t)) & \text{for } t_0 \le t < t_1 \\ R_y\left(-\frac{\pi}{2}\right)R_x(-\beta_{②}(t)) & \\ \quad \times\ \omega_\epsilon I_x R_x(\beta_{②}(t))R_y\left(\frac{\pi}{2}\right) & \text{for } t_1 \le t < t_2 \\ R_x(-\pi)R_y\left(-\beta_{③}(t) + \frac{\pi}{2}\right) & \\ \quad \times \omega_\epsilon I_y R_y\left(\beta_{③}(t) - \frac{\pi}{2}\right)R_x(\pi) & \text{for } t_2 \le t \le t_3. \end{cases} \tag{79}$$

This can readily simplified since the spin operators and rotation operators commute in most of the cases:

$$\tilde{H}_B(t) = \begin{cases} \tilde{H}_B^{①} = \omega_\epsilon I_y & \text{for } t_0 \le t < t_1 \\ \tilde{H}_B^{②} = \omega_\epsilon I_z & \text{for } t_1 \le t < t_2 \\ \tilde{H}_B^{③} = -\omega_\epsilon I_y & \text{for } t_2 \le t \le t_3, \end{cases} \tag{80}$$

where we have introduced the shorthand notation $\tilde{H}_B^{①}$, $\tilde{H}_B^{②}$ and $\tilde{H}_B^{③}$ for the three time-independent interaction frame Hamiltonians during blocks ①, ②, and ③ of the composite pulse. Hence, we note that the final interaction frame Hamiltonian is piecewise time-independent, a case generally discussed in Section 3.1.

4.1.4 | First order average Hamiltonian and propagator

After we have determined the interaction frame Hamiltonian in Equation 80, it is now time to calculate the first order average Hamiltonian according to Equations 30 and 44:

$$\begin{aligned} \bar{H}_B^{(1)} &= \frac{1}{T}\int_{t_0}^{t_3} \mathrm{d}t\ \tilde{H}(t) \\ &= \frac{1}{T}\left\{\tilde{H}_B^{①}\tau_1 + \tilde{H}_B^{②}\tau_2 + \tilde{H}_B^{③}\tau_3\right\} \\ &= \frac{1}{4}\omega_\epsilon I_y + \frac{1}{2}\omega_\epsilon I_z - \frac{1}{4}\omega_\epsilon I_y \\ &= \frac{1}{2}\omega_\epsilon I_z \end{aligned} \tag{81}$$

This is the first order average Hamiltonian in the interaction frame of the rf field. Hence, the resulting *total* propagator $U(t_3, t_0)$ over the whole composite pulse is according to Equation 57 to first order average Hamiltonian theory given by the product of $U_A(t_3, t_0)$ and the propagator $\bar{U}_B(t_3, t_0) = \exp\{-i\bar{H}_B^{(1)}T\}$:

$$
\begin{aligned}
U(t_3,t_0) &\approx U_A(t_3,t_0)\bar{U}_B(t_3,t_0)\\
&= U_A(t_3,t_0)\exp\{-i\bar{H}_B^{(1)}T\}\\
&= R_x(\pi)R_z\left(\frac{1}{2}\omega_\epsilon T\right)\\
&= R_x(\pi)R_z(\pi\epsilon),
\end{aligned}
\tag{82}
$$

where we used the relative amplitude error $\epsilon = \omega_\epsilon/\omega_{\text{nut}}$, and the relationship $\omega_{\text{nut}}T = 2\pi$. The final propagator is a product of two rotations, first a rotation around the z-axis by $\pi\epsilon$, which depends on the relative amplitude error, and second the ideal rotation by π around the x-axis, which corresponds to a 180_x pulse. Hence, under the $90_y180_x90_y$ composite pulse, inversion of longitudinal magnetization is compensated for rf amplitude errors in first order average Hamiltonian theory, whereas transverse magnetization acquires a phase with value $-\pi\epsilon$ in the xy-plane under inversion.

To illustrate this, Figure 9 shows the results of calculating the trajectory of three density operators $\rho_0 = I_z$, I_x and I_y, corresponding to z-, x-, and y-magnetization, during a single 180_x pulse and during the $90_y180_x90_y$ composite pulse in the presence of relative amplitude errors of $\epsilon = -5\%$ (A-C) and -15% (D-F). The density operator after the propagation under the sequence of pulses is labeled ρ_1. The graphs were plotted with the help of Malcolm H. Levitt's Mathematica[42] package *mPackages* (version 4.30), the predecessor of *SpinDynamica*.[43]

Let's start by having a closer look at the left panel (A-C), showing the results for an amplitude error of $\epsilon = -5\%$,

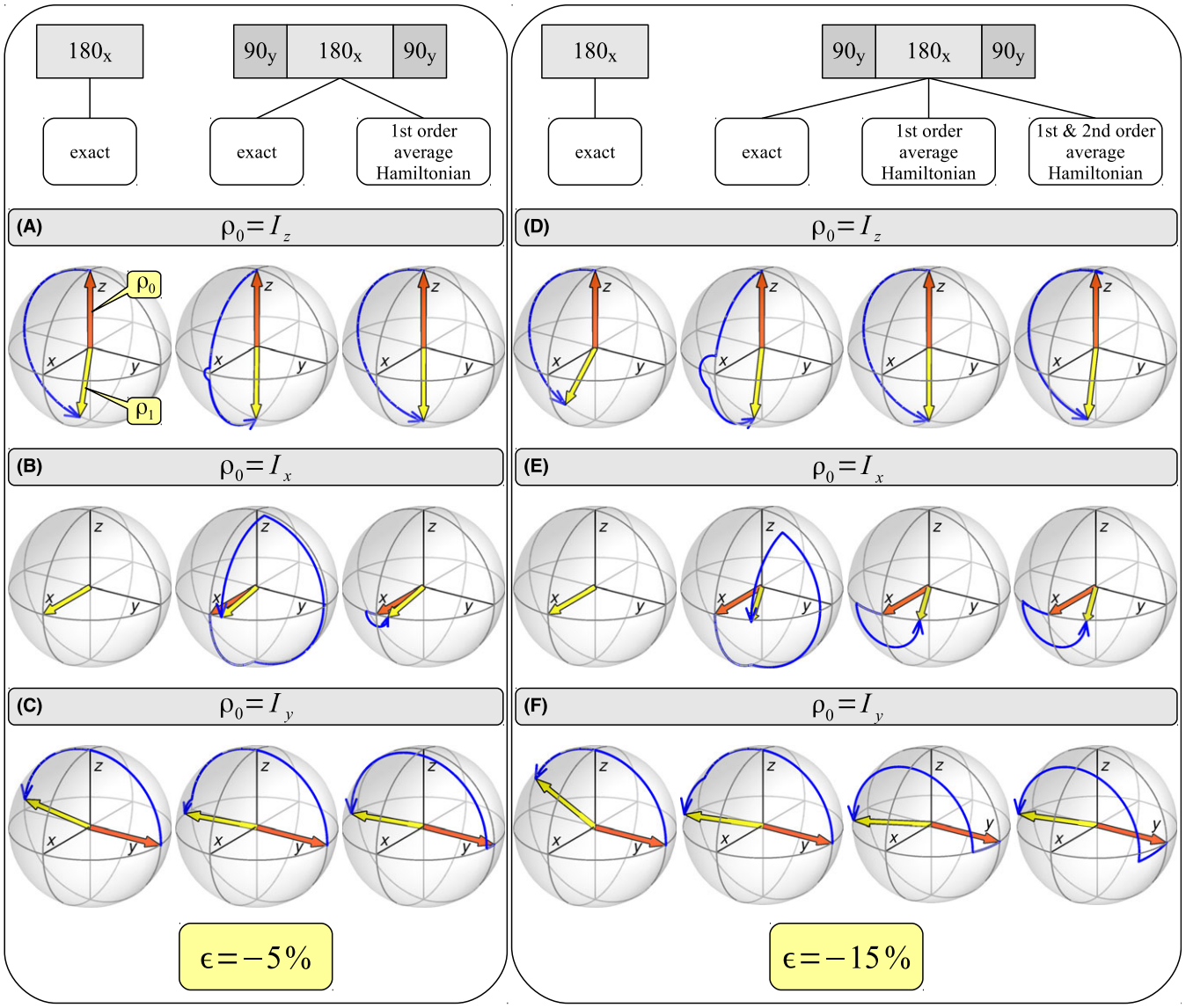

FIGURE 9 Trajectories of z-, x-, and y-magnetization vectors during a single 180_x pulse and during the $90_y180_x90_y$ composite pulse in the presence of relative rf amplitude errors ϵ of -5% and -15%. Details are discussed in the text

and in particular the first row (A) that shows the trajectory of a z-magnetization vector ($\rho_0 = I_z$). Since the rf amplitude is set slightly too small, the z-magnetization is not completely inverted under a single 180_x pulse, as can be seen on the left. The panel in the middle shows the exact trajectory the z-magnetization takes during the $90_y180_x90_y$ composite pulse, leading to perfect inversion in spite of the misset of the rf amplitude ($\rho_1 = -I_z$). This graph elucidates the mechanism of compensation for rf amplitude errors: The first 90_y pulse rotates the z-magnetization vector to a position slightly above the x-axis, since the rf amplitude error causes the flip angle to be slightly less than 90°. The following 180_x pulse rotates the magnetization slightly below the xy-plane, however, because of the amplitude error, the final position is not exactly below the x-axis. Finally, the last 90_y pulse rotates the magnetization vector to a position that is almost perfectly along the $-z$-axis, as its flip angle is again slightly less than 90°.

The trajectory under the propagator in first order average Hamiltonian theory is shown on the right: it corresponds to a perfect inversion of the z-magnetization vector. It is important to remind the reader that the propagator based on the average Hamiltonian strictly may be used solely to calculate the *final* density operator ρ_1 after the pulse sequence, it does not provide any insight into the actual trajectory of the spin system *during* the sequence of pulses, as is evident by comparing the exact trajectories with the ones based on average Hamiltonian theory in Figure 9.

The second row (B) in the left panel of Figure 9 shows the trajectory of an x-magnetization vector ($\rho_0 = I_x$). As expected a single 180_x pulse does not result in any rotation, ie, $\rho_1 = \rho_0 = I_x$, shown on the left. More interesting is the exact trajectory of the x-magnetization under the $90_y180_x90_y$ composite pulse. The small rf amplitude error causes the final magnetization vector to lie in the xy-plane enclosing a small angle with the x-axis, given by $-\pi\epsilon = 9°$. The final density operator ρ_1 is nicely reproduced by the trajectory under the propagator in first order average Hamiltonian theory, as shown on the right.

Finally, the different trajectories of y-magnetization are show in row (C) in the left panel of Figure 9. Due to the small rf amplitude error the single 180_x pulse does not invert the y-magnetization entirely, rather the magnetization vector stops above, short of the $-y$-axis. In contrast, after the $90_y180_x90_y$ composite pulse, the final magnetization vector lies in the xy-plane, enclosing the small angle of 9° as discussed above with the $-y$-axis. The same final density operator is reproduced in first order average Hamiltonian theory as shown on the right.

So far, the relative amplitude error ϵ has been small enough, so that first order average Hamiltonian theory proved to be sufficient for calculating the propagator over the composite pulse satisfactory when comparing the results with exact calculations. However, in the following we want to turn our attention to the results shown in the right panel (D-F) of Figure 9 for an amplitude error of $\epsilon = -15\%$, in which case first order average Hamiltonian theory will be shown to be insufficient.

The first row (D) shows the trajectory of a starting density operator I_z (z-magnetization). The larger rf amplitude misset causes the final position of the magnetization vector to clearly fall short of the $-z$-axis for a single 180_x pulse. Interestingly, also the $90_y180_x90_y$ composite pulse fails to perfectly invert the z-magnetization, however the resulting error is smaller than in the case of the single 180_x pulse. However, the first order average Hamiltonian does still cause a perfect inversion of the z-magnetization. We can conclude that for a relative rf amplitude error of $\epsilon = -15\%$ first order average Hamiltonian theory is not sufficient to calculate the propagator under the $90_y180_x90_y$ composite pulse satisfactory. Hence, in the following section we will go a step further and calculate the second order average Hamiltonian for the $90_y180_x90_y$ composite pulse in the presence of an rf amplitude error.

4.1.5 | Second order average Hamiltonian and propagator

Since the interactions frame Hamiltonian in Equation 80 is piecewise time-independent we can calculate the second order average Hamiltonian as outlined in Section 3.1, ie, we solely have to include commutators of the interaction frame Hamiltonian during *pairwise different* blocks (①, ② or ③) of the composite pulse, see Equation 45:

$$\begin{aligned}\bar{H}_B^{(2)} &= \frac{1}{2\mathrm{i}T}\int_{t_0}^{t_3}\mathrm{d}t\int_{t_0}^{t}\mathrm{d}t'[\tilde{H}(t),\tilde{H}(t')]\\ &= \frac{1}{2\mathrm{i}T}\Big\{[\tilde{H}_B^{②},\tilde{H}_B^{①}]\tau_2\tau_1 + \underbrace{[\tilde{H}_B^{③},\tilde{H}_B^{①}]}_{=0}\tau_3\tau_1 + [\tilde{H}_B^{③},\tilde{H}_B^{②}]\tau_3\tau_2\Big\}\\ &= \frac{T}{16\mathrm{i}}\Big\{[\tilde{H}_B^{②},\tilde{H}_B^{①}] + [\tilde{H}_B^{③},\tilde{H}_B^{②}]\Big\}\\ &= \frac{T}{16\mathrm{i}}\omega_\epsilon^2\Big\{[I_z,I_y] - [I_y,I_z]\Big\}\\ &= -\frac{\pi}{4}\frac{\omega_\epsilon^2}{\omega_{\mathrm{nut}}}I_x,\end{aligned} \tag{83}$$

where we have made extensive use of the definitions and relationships of time intervals during the composite pulse given in Equation 71 and above. Furthermore, we used the commutator relationship $[I_y, I_z] = \mathrm{i}I_x$. To gain further insight into the significance of the second order average

Hamiltonian in the rf interaction frame, we collect the first and second order results, Equations 81 and 83, respectively, to arrive at the total propagator $U(t_3,\ t_0)$ over the whole composite pulse in second order average Hamiltonian theory:

$$\begin{aligned} U(t_3,t_0) &\approx U_A(t_3,t_0)\bar{U}_B(t_3,t_0) \\ &= R_x(\pi)\exp\{-\mathrm{i}(\bar{H}_B^{(1)}+\bar{H}_B^{(2)})T\} \\ &= R_x(\pi)\exp\left\{-\mathrm{i}T\left(\frac{1}{2}\omega_\epsilon I_z-\frac{\pi}{4}\frac{\omega_\epsilon^2}{\omega_{\mathrm{nut}}}I_x\right)\right\} \\ &= R_x(\pi)\exp\left\{-\mathrm{i}\left(\pi\epsilon I_z-\frac{1}{2}\pi^2\epsilon^2 I_x\right)\right\} \\ &= R_x(\pi)\exp\{-\mathrm{i}\beta_{\mathrm{eff}}(I_z\cos\theta-I_x\sin\theta)\}, \end{aligned} \tag{84}$$

where the exponential operator in the last line represents a rotation about an axis in the $-xz$-plane that encloses the angle $\theta = \arctan(\pi\epsilon/2)$ with the z-axis by the flip angle $\beta_{\mathrm{eff}} = \pi\epsilon\sqrt{1+\pi^2\epsilon^2/4}$. We can perform a consistency check of this result comparing it with the first order average Hamiltonian propagator: If $\pi\epsilon$ is sufficiently small, we get $\beta_{\mathrm{eff}} \approx \pi\epsilon$, $\cos\ \beta_{\mathrm{eff}} \approx 1$ and $\sin\ \beta_{\mathrm{eff}} \approx 0$, consequently arriving back at the result in Equation 82.

Now we can revisit the results shown in the right panel (D-F) of Figure 9 for an amplitude error of $\epsilon = -15\%$. In Section 4.1.4 we saw that the propagator for the $90_y180_x90_y$ composite pulse in first order average Hamiltonian theory was not able to correctly generate the final position of the magnetization vector starting from z-magnetization, ($\rho_0 = I_z$) as can be seen in the third column of the first row (D). However, the last column shows the trajectory under the propagator in second order average Hamiltonian theory starting from z-magnetization. It is evident that the final position reached by the magnetization vector resembles very well the final position after the exact trajectory during the $90_y180_x90_y$ composite pulse.

The second row (E) in the right panel of Figure 9 shows the trajectories of x-magnetization. A single 180_x pulse even with an amplitude error has no influence, hence the starting and finishing magnetization vectors are identical, as shown in the left column. The exact trajectory of x-magnetization during the $90_y180_x90_y$ composite pulse is depicted in the second columns, it finishes with the magnetization vector lying in the xy-plane enclosing an angle of about $-\pi\epsilon = 27°$ with the x-axis. We note that this specific result can already very well be predicted by employing the propagator in first average Hamiltonian theory as is shown in the third column. Hence, the trajectory using second order average Hamiltonian theory, shown in the right column, is almost indistinguishable from the one using first order theory.

The last row (C) in the left panel of Figure 9 shows the different trajectories of y-magnetization. Due to the larger amplitude error, a single 180_x pulse fails clearly to invert y-magnetization, leading to a final magnetization vector well above the $-y$-axis. The exact trajectory of y-magnetization under the $90_y180_x90_y$ composite pulse leads the magnetization vector to its final position in the xy-plane, enclosing a small angle with the $-y$-axis, as can be seen in the second column. Interestingly, in first order average Hamiltonian theory the final magnetization vector encloses a larger angle with the $-y$-axis (third column), not in agreement with the result of the exact trajectory. However, the propagator in second order average Hamiltonian theory, leads to a final position that is in agreement with the result of the exact trajectory.

Concluding this section, we could show that for a larger error in the rf amplitude of $\epsilon = -15\%$ the propagator in second order average Hamiltonian theory was sufficient to reproduce satisfactory the final magnetization vectors compared to the exact propagation.

4.2 | The composite pulse $90_y270_x90_y$

In the previous section we have used average Hamiltonian theory to show that the $90_y180_x90_y$ composite pulse is compensated with respect to rf amplitude errors if employed as an inversion pulse of longitudinal magnetization. However, an important application of average Hamiltonian theory is not only to understand existing pulse sequences, but also to *design* pulse sequences with certain desired properties. In this section we want to demonstrate how to *design* a simple composite pulse that is compensated with respects to the rf frequency offset using first order average Hamiltonian theory. We will start with a slight modification of the previous $90_y180_x90_y$ pulse that allows a single degree of freedom to be optimized for the targeted compensation property: $90_y\beta_x90_y$, where β is the flip angle parameter, which should be optimized such that the resulting composite pulse is compensated in first order average Hamiltonian theory with respect to rf frequency offsets.

Figure 8B shows the timings of the $90_y\beta_x90_y$ composite pulse. The durations of the individual pulses ①, ②, and ③ are given by $\tau_1 = t_1 - t_0$, $\tau_2 = t_2 - t_1$, $\tau_3 = t_3 - t_2$, respectively. The total duration is given by $T = t_3 - t_1 = \tau_1 + \tau_2 + \tau_3$, and the following relationships are satisfied:

$$\begin{aligned} \omega_{\mathrm{nut}}\tau_1 &= \omega_{\mathrm{nut}}\tau_3 = \frac{\pi}{2} \\ \omega_{\mathrm{nut}}\tau_2 &= \beta \\ \omega_{\mathrm{nut}}T &= \pi+\beta, \end{aligned} \tag{85}$$

where ω_{nut} is the ideal nutation frequency of the rf field during the composite pulse.

4.2.1 | Hamiltonian

If we consider again a single *I*-spin system, its Hamiltonian at time point t in the presence of the Zeeman interaction and the interaction with the rf field during the composite pulse, including an rf frequency offset, in the high-field approximation and in the rotating reference frame is given by, according to Equation 21:

$$\begin{aligned} H(t) &= \omega_{\text{nut}}(I_x \cos\phi(t) + I_y \sin\phi(t)) + \Delta I_z \\ &= \underbrace{\omega_{\text{nut}} R_z(\phi(t)) I_x R_z(-\phi(t))}_{H_A(t)} + \underbrace{\Delta I_z}_{H_B(t)} \end{aligned}, \tag{86}$$

where Δ is the rf resonance frequency offset, and $\phi(t)$ is the rf phase at time point t during the composite pulse. In the last line we have split the Hamiltonian into two parts, $H_A(t)$ is the time-dependent Hamiltonian of the interaction with the ideal rf field and $H_B(t)$ is the time-independent Hamiltonian of the rf resonance offset. If the ratio $\Delta/\omega_{\text{nut}}$ is relatively small, it is helpful to transform $H(t)$, and hence $H_B(t)$, into the interaction frame of $H_A(t)$ as discussed in Section 3.2. Since $H_A(t)$ is Hamiltonian of the interaction with the on-resonance rf field, the interaction frame in this case is also referred to as the "toggling frame" as discussed in Section 3.2. In order to achieve the transformation, in a first step we list $H_A(t)$ and $H_B(t)$ during the different pulse sequence blocks ①, ② and ③:

$$H_A(t) = \begin{cases} \omega_{\text{nut}} I_y & \text{for} \quad t_0 \le t < t_1 \text{ or } t_2 \le t \le t_3 \\ \omega_{\text{nut}} I_x & \text{for} \quad t_1 \le t < t_2 \end{cases} \tag{87}$$

and

$$H_B(t) = \Delta I_z \qquad \text{for} \quad t_0 \le t \le t_3 \tag{88}$$

4.2.2 | Rf propagator

In a second step we need to calculate the propagator $U_A(t, t_0)$ for the Hamiltonian that solves the Schrödinger equation (Equation 50) of the Hamiltonian $H_A(t)$. The propagator during the three time blocks ①, ② and ③ is given by:

$$U_A(t, t_0) = \begin{cases} R_y(\omega_{\text{nut}}(t - t_0)) & \text{for} \quad t_0 \le t < t_1 \\ R_x(\omega_{\text{nut}}(t - t_1)) R_y\left(\frac{\pi}{2}\right) & \text{for} \quad t_1 \le t < t_2 \\ R_y(\omega_{\text{nut}}(t - t_2)) R_x(\beta) R_y\left(\frac{\pi}{2}\right) & \text{for} \quad t_2 \le t \le t_3. \end{cases} \tag{89}$$

Note again how the propagators accumulate from right to left in the second and third line, see also Equation 4. As in Section 4.1.2 we use the relationships $\beta_①(t) = \omega_{\text{nut}}(t - t_0)$, $\beta_②(t) = \omega_{\text{nut}}(t - t_1)$ and $\beta_③(t) = \omega_{\text{nut}}(t - t_2)$ to simplify the propagator expression:

$$U_A(t, t_0) = \begin{cases} R_y(\beta_①(t)) & \text{for } t_0 \le t < t_1 \\ R_x(\beta_②(t)) R_y\left(\frac{\pi}{2}\right) & \text{for } t_1 \le t < t_2 \\ R_y\left(\beta_③(t) + \frac{\pi}{2}\right) R_z(\beta) & \text{for } t_2 \le t \le t_3, \end{cases} \tag{90}$$

where we used in the last line the transformation

$$R_x(\beta) R_y\left(\frac{\pi}{2}\right) = R_y\left(\frac{\pi}{2}\right) R_y\left(-\frac{\pi}{2}\right) R_x(\beta) R_y\left(\frac{\pi}{2}\right) = R_y\left(\frac{\pi}{2}\right) R_z(\beta). \tag{91}$$

In order to transform the Hamiltonian into the interaction frame we also need to calculate the adjoint of the rf propagator:

$$U_A^\dagger(t, t_0) = \begin{cases} R_y(-\beta_①(t)) & \text{for } t_0 \le t < t_1 \\ R_y\left(-\frac{\pi}{2}\right) R_x(-\beta_②(t)) & \text{for } t_1 \le t < t_2 \\ R_z(-\beta) R_y\left(-\beta_③(t) - \frac{\pi}{2}\right) & \text{for } t_2 \le t \le t_3. \end{cases} \tag{92}$$

4.2.3 | Interaction frame Hamiltonian

We can now employ the rf propagator $U_A(t, t_0)$ calculated in the previous section to transform the Hamiltonian into the interaction frame of $H_A(t)$ ("toggling frame") according to Equation 56:

$$\tilde{H}_B(t) = \begin{cases} R_y(-\beta_①(t)) \Delta I_z R_y(\beta_①(t)) & \text{for} \quad t_0 \le t < t_1 \\ R_y\left(-\frac{\pi}{2}\right) R_x(-\beta_②(t)) & \\ \quad \times \Delta I_z R_x(\beta_②(t)) R_y\left(\frac{\pi}{2}\right) & \text{for} \quad t_1 \le t < t_2 \\ R_z(-\beta) R_y\left(-\beta_③(t) - \frac{\pi}{2}\right) & \\ \quad \times \Delta I_z R_y\left(\beta_③(t) + \frac{\pi}{2}\right) R_z(\beta) & \text{for} \quad t_2 \le t \le t_3. \end{cases} \tag{93}$$

The first rotations around the *y*- and *x*-axis in the first and second line, respectively, of Equation 93 are relatively straightforward to execute, whereas in the case of the last row we use the relationships $\cos\left(\frac{\pi}{2} + x\right) = -\sin x$ and $\sin\left(\frac{\pi}{2} + x\right) = \cos x$ after the *y*-rotation:

$$\tilde{H}_B(t) = \begin{cases} \Delta\{I_z \cos\beta_①(t) - I_x \sin\beta_①(t)\} & \text{for} \quad t_0 \le t < t_1 \\ \Delta R_y\left(-\frac{\pi}{2}\right)\{I_z \cos\beta_②(t) & \\ \quad + I_y \sin\beta_②(t)\} R_y\left(\frac{\pi}{2}\right) & \text{for} \quad t_1 \le t < t_2 \\ \Delta R_z(-\beta)\{-I_z \sin\beta_③(t) & \\ \quad - I_x \cos\beta_③(t)\} R_z(\beta) & \text{for} \quad t_2 \le t \le t_3. \end{cases} \tag{94}$$

Finally, the remaining rotations in the second and last line are carried out:

$$\tilde{H}_B(t) = \begin{cases} \Delta\{I_z \cos\beta_①(t) - I_x \sin\beta_①(t)\} & \text{for} \quad t_0 \le t < t_1 \\ \Delta\{-I_x \cos\beta_②(t) + I_y \sin\beta_②(t)\} & \text{for} \quad t_1 \le t < t_2 \\ \Delta\{-I_z \sin\beta_③(t) & \\ \quad + (I_y \sin\beta - I_x \cos\beta) \cos\beta_③(t)\} & \text{for} \quad t_2 \le t \le t_3. \end{cases} \tag{95}$$

This result is more complicated than the one we got in Section 4.1.3, here the resulting interaction frame Hamiltonian is not piecewise time-independent during the different pulse blocks.

4.2.4 | First order average Hamiltonian

With the help of the interaction frame Hamiltonian in Equation 95, we can now calculate the first order average Hamiltonian according to Equation 30:

$$\begin{aligned}\bar{H}_B^{(1)} &= \frac{1}{T}\int_{t_0}^{t_3} \mathrm{d}t\ \tilde{H}(t) \\ &= \frac{1}{\pi+\beta}\left\{\underbrace{\int_0^{\frac{\pi}{2}} \mathrm{d}\beta_{①}\tilde{H}_B^{①}(\beta_{①})}_{\int_{①}} + \underbrace{\int_0^{\beta} \mathrm{d}\beta_{②}\tilde{H}_B^{②}(\beta_{②})}_{\int_{②}} + \underbrace{\int_0^{\frac{\pi}{2}} \mathrm{d}\beta_{③}\tilde{H}_B^{③}(\beta_{③})}_{\int_{③}}\right\},\end{aligned} \tag{96}$$

where we have substituted the integration over the time variable t with the integration over the flip angles $\beta_{①}$, $\beta_{②}$ and $\beta_{③}$ during the three blocks ①, ②, and ③, respectively. Hence, the normalizing by the total duration T is replaced by the normalization by the sum of the flip angles $\pi + \beta$ of the composite pulse. In addition, we have used the shorthand notations $\tilde{H}_B^{①}(\beta_{①})$, $\tilde{H}_B^{②}(\beta_{②})$ and $\tilde{H}_B^{③}(\beta_{③})$ for the interaction frame Hamiltonians during the different blocks in Equation 95. The three integrals $\int_{①}$, $\int_{②}$ and $\int_{③}$ can be solved separately:

$$\begin{aligned}\int_{①} &= \Delta\left[I_z \sin\beta_{①} + I_x \cos\beta_{①}\right]_0^{\frac{\pi}{2}} \\ &= \Delta\{I_z - I_x\} \\ \int_{②} &= \Delta\left[-I_x \sin\beta_{②} - I_y \cos\beta_{②}\right]_0^{\beta} \\ &= \Delta\{-I_x \sin\beta + I_y(1-\cos\beta)\} \\ \int_{③} &= \Delta\left[I_z \cos\beta_{③} + \left(I_y \sin\beta - I_x \cos\beta\right)\sin\beta_{③}\right]_0^{\frac{\pi}{2}} \\ &= \Delta\{-I_z + I_y \sin\beta - I_x \cos\beta\},\end{aligned} \tag{97}$$

which finally leads to the first order average Hamiltonian

$$\bar{H}_B^{(1)} = \frac{\Delta}{\pi+\beta}\{-I_x(1+\sin\beta+\cos\beta) + I_y(1-\cos\beta+\sin\beta)\}. \tag{98}$$

The goal of this section is to choose the flip angle β of pulse ② such that the resulting composite pulse is compensated for rf frequency offsets in first order average Hamiltonian theory. This would imply we would like to achieve that $\bar{H}_B^{(1)}$ is zero for our choice of β:

$$\bar{H}_B^{(1)} = 0 \quad \text{if} \quad \begin{array}{l} 1+\sin\beta+\cos\beta = 0 \\ \wedge\ 1-\cos\beta+\sin\beta = 0 \end{array} \Leftrightarrow \begin{array}{l} \sin\beta = -1 \\ \wedge\ \cos\beta = 0 \end{array} \tag{99}$$

The simple equation system in the right column of Equation 99 is solved straightforwardly by $3\pi/2$ plus any multiple of 2π. We can summarize this condition in the following equation:

$$\bar{H}_B^{(1)} = 0 \qquad \text{if} \qquad \beta = \frac{3\pi}{2} + Z2\pi, \quad \text{where } Z \text{ is any integer} \tag{100}$$

Hence, for example the $90_y270_x90_y$ composite pulse would be an inversion pulse that is compensated with respect to rf frequency offsets. However, we need to carefully check whether the $90_y270_x90_y$ composite pulse actually is equivalent to a 180_x pulse under ideal circumstances (no rf offset). As it is proven in Appendix A this is not the case, rather it is equivalent to a 180_{-45} pulse. However, as a result, the $90_{135}270_{45}90_{135}$ composite pulse is indeed equivalent to a 180_x pulse.

In Figure 10 the operation of the $90_{135}270_{45}90_{135}$ composite pulse is demonstrated by following the trajectories of z-, x-, and y-magnetization during the composite pulse in the presence of a relative rf frequency offset of $\Delta/\omega_{\mathrm{nut}} = 10\%$. The trajectories shown in first row (A) start with the density operator $\rho_0 = I_z$, corresponding to z-magnetization. The left panel shows that a single 180_x pulse cannot perfectly invert the z-magnetization vector due to rf offset. The exact trajectory of the magnetization vector during the $90_{135}270_{45}90_{135}$ pulse shown in the middle panel is very interesting and leads to a completely inverted z-magnetization vector. The propagator of the $90_{135}270_{45}90_{135}$ composite pulse corresponds to a $R_x(\pi)$ rotation operator in first order average Hamiltonian theory, hence z-magnetization is perfectly inverted in first order average Hamiltonian theory as depicted in the right panel.

The second row (B) in Figure 10 shows the trajectories of x-magnetization. The presence of the rf frequency offset causes the single 180_x pulse to lift the final position of the x-magnetization vector slightly above the x-axis, shown on the left. The exact trajectory of the x-magnetization during the $90_{135}270_{45}90_{135}$ composite pulse is quite complicated, but nevertheless leads right back onto the x-axis, as expected for a pulse compensated for rf frequency offsets, as shown in the middle panel. Since in first order average Hamiltonian theory, the $90_{135}270_{45}90_{135}$ composite pulse is identical to a 180_x pulse, even in the presence of rf frequency offsets, the x-magnetization vector remains in its position.

Finally, the last row (C) in Figure 10 depicts the different trajectories of a starting I_y density operator, corresponding to y-magnetization. As shown in the left panel, in spite of the rf offset the trajectory during the single 180_x pulse follows closely one without rf offset. As expected, the

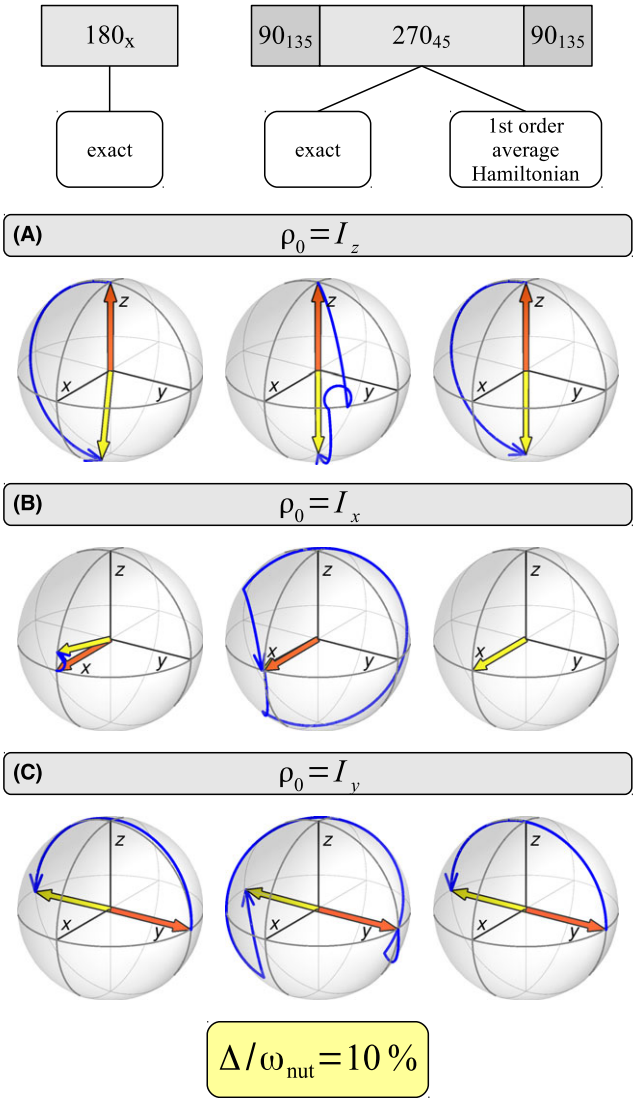

FIGURE 10 Trajectories of *z*-, *x*-, and *y*-magnetization vectors during a single 180_x pulse and during the $90_{135}270_{45}90_{135}$ composite pulse in the presence of a relative rf frequency offset of $\Delta/\omega_{nut} = 10\%$. Details are discussed in the text

$90_{135}270_{45}90_{135}$ composite pulse inverts perfectly the *y*-magnetization vector in the presence of a small rf offset, as does the propagator $R_x(\pi)$ of the composite pulse in first order average Hamiltonian theory, shown in the middle and right panels, respectively.

5 | CONCLUDING REMARKS

In this first part of our introduction to average Hamiltonian theory, our goal was to introduce the basics of this topic in a comprehensive but rigorous fashion. The two composite pulses were chosen as examples to familiarize the reader with applying the concept of the interaction frame and the Magnus expansion in practice. The reader is encouraged to consult Edén's recent educational papers in this journal on the Zeeman truncation in NMR for another important example of applying average Hamiltonian theory in the interaction frame.[38,39] Finally, part II of this introduction to average Hamiltonian theory will cover more advanced examples, such as dipolar recoupling and homonuclear decoupling in solid-state NMR, of the application of average Hamiltonian theory in NMR.

ACKNOWLEDGMENTS

I would like to thank Malcolm Levitt for introducing me to the exciting world of average Hamiltonian theory during my time as PhD student in his laboratory at that time at Stockholm University. As this paper emerged from educational lectures given at conferences and summer schools, I am grateful to valuable comments by some of the other lectures, specifically Marc Baldus, Matthias Ernst, Bob Griffin, Beat Meier, Niels Nielsen, Shimon Vega and Thomas Vosegaard. Finally, I would like to thank the anonymous reviewer who suggested to consider the non-cyclic case for periodic Hamiltonians.

ORCID

Andreas Brinkmann http://orcid.org/0000-0001-6442-3780

REFERENCES

1. Chechik V, Carter E, Murphy D. *Electron Paramagnetic Resonance*. New York, NY: Oxford University Press; 2016.
2. Ernst RR, Bodenhausen G, Wokaun A. *Principles of Nuclear Magnetic Resonance in One and Two Dimensions*. No. 14 in International Series of Monographs on Chemistry, Oxford, UK: Oxford University Press; 1997.
3. Levitt MH. *Spin Dynamics: Basics of Nuclear Magnetic Resonance*, 2nd edn. Chichester, UK: Wiley; 2008.
4. Vega AJ. Quadrupolar nuclei in solids. *eMagRes*. 2010; https://doi.org/10.1002/9780470034590.emrstm0431.pub2.
5. Bushong SC, Clarke G. *Magnetic Resonance Imaging: Physical & Biological Principles*, 4th edn. St. Louis, MO: Mosby; 2014.
6. Yannoni CS, Züger O, Rugar D, Sidles JA. Force detection and imaging in magnetic resonance. *eMagRes*. 2007. https://doi.org/10.1002/9780470034590.emrstm0174
7. Haeberlen U, Waugh JS. Coherent averaging effects in magnetic resonance. *Phys Rev*. 1968;175:453-467.
8. Haeberlen U. *High Resolution NMR in Solids. Selective Averaging. Advances in Magnetic Resonance*, Supplement 1. New York, NY: Academic Press; 1976.
9. Waugh JS. Average Hamiltonian theory. In: Grant DM, Harris RK, eds. *Encyclopedia of Nuclear Magnetic Resonance*, vol. 2. Chichester, UK: Wiley; 1996:849-854.
10. Mehring M. *Principles of High Resolution NMR in Solids*, 2nd edn. Berlin, Germany: Springer-Verlag; 1983.
11. Magnus W. On the exponential solution of differential equations for a linear operator. *Commun Pure Appl Math*. 1954;7:649-673.

12. Levitt MH. Composite pulses. *Prog Nucl Mag Res Sp*. 1986;18:61-122.
13. Levitt MH. Composite pulses. In: Grant DM, Harris RK, eds. *Encyclopedia of Nuclear Magnetic Resonance*, vol. 2. Chichester, UK: Wiley; 1996:1396-1411.
14. Tycko R. Iterative methods in the design of pulse sequences for NMR excitation. In: Waugh JS, ed. *Advances in Magnetic and Optical Resonance*, vol. 15. New York, NY: Academic Press; 1990: 1-49.
15. Bennett AE, Griffn RG, Vega S. Recoupling of homo- and heteronuclear and heteronuclear dipolar interactions in rotating solids. *NMR Basic Princ Prog*. 1994;33:1-77.
16. Dusold S, Sebald A. Dipolar recoupling under magic-angle spinning conditions. *Ann Rep NMR Spectrosc*. 2000;41:185-264.
17. Edén M. Advances in symmetry-based pulse sequences in magic-angle spinning solidstate NMR. *eMagRes*. 2013;2:351-364.
18. Sakurai JJ. *Modern Quantum Mechanics*. New-York, NY: Addison-Wesley; 1994.
19. Cohen-Tannoudji C, Diu B, Laloë F. *Quantum Mechanics*. New York, NY: Wiley; 1977.
20. Messiah A. *Quantum Mechanics*. Mineola, NY: Dover; 1999.
21. Smith SA, Palke WE, Gerig JT. The Hamiltonians of NMR. Part I. *Concepts Magn Reson*. 1992;4:107-144.
22. Smith SA, Palke WE, Gerig JT. The Hamiltonians of NMR. Part II. *Concepts Magn Reson*. 1992;4:181-204.
23. Smith SA, Palke WE, Gerig JT. The Hamiltonians of NMR. Part III. *Concepts Magn Reson*. 1993;5:151-177.
24. Smith SA, Palke WE, Gerig JT. The Hamiltonians of NMR. Part IV: NMR relaxation. *Concepts Magn Reson*. 1994;6:137-162.
25. Maricq MM, Waugh JS. NMR in rotating solids. *J Chem Phys*. 1979;70:3300-3316.
26. Edén M. Computer simulations in solid-state NMR. I. Spin dynamics theory. *Concepts Magn Reson A*. 2003;17A:117-154.
27. Edén M. Computer simulations in solid-state NMR. II. Implementations for static and rotating samples. *Concepts Magn Reson A*. 2003;18A:1-23.
28. Edén M. Computer simulations in solid-state NMR. III. Powder averaging. *Concepts Magn Reson A*. 2003;18A:24-55.
29. Vega S. Floquet theory. In: Grant DM, Harris RK, eds. *Encyclopedia of Nuclear Magnetic Resonance*, vol. 3. Chichester, UK: Wiley; 2011:2011-2025.
30. Bain AD, Dumont RS. Introduction to Floquet theory: The calculation of spinning sideband intensities in magic-angle spinning NMR. *Concepts Magn Reson*. 2001;13:159-170.
31. Wilcox RM. Exponential operators and parameter differentiation in quantum physics. *J Math Phys*. 1967;8:962-982.
32. Bialynicki-Birula I, Mielnik B, Plebański J. Explicit solution of the continuous Baker-Campbell-Hausdorff problem and a new expression for the phase operator. *Ann Phys*. 1969;51:187-200.
33. Klarsfeld S, Oteo JA. Recursive generation of higher-order terms in the Magnus expansion. *Phys Rev A*. 1989;39:3270-3273.
34. Mansfield P. Symmetrized pulse sequences in high resolution NMR in solids. *J Phys C*. 1971;4:1444-1452.
35. Burum DP. Magnus expansion generator. *Phys Rev B*. 1981;24: 3684-3692.
36. Hahn EL. Spin echoes. *Phys Rev*. 1950;80:580-594.
37. Jeener J. Emphasizing the role of time in quantum dynamics. *Bull Magn Reson*. 1994;16:35-42.
38. Edén M. Zeeman truncation in NMR. I. The role of operator commutation. *Concepts Magn Reson A*. 2014;43:91-108.
39. Edén M. Zeeman truncation in NMR. II. Time averaging in the rotating frame. *Concepts Magn Reson A*. 2014;43:109-126.
40. Caravatti P, Bodenhausen G, Ernst RR. Selective pulse experiments in high-resolution solid state NMR. *J Magn Reson*. 1983;55:88-103.
41. Levitt MH, Freeman R. NMR population inversion using a composite pulse. *J Magn Reson*. 1979;33:473-476.
42. Wolfram Research Inc. *Mathematica (Version 10.0.2)*. Champaign, IL: Wolfram Research Inc.; 2014.
43. Bengs C, Levitt MH. SpinDynamica: Symbolic and numerical magnetic resonance in a Mathematica environment. *Magn Reson Chem*. 2017;147:296.

How to cite this article: Brinkmann A. Introduction to average Hamiltonian theory. I. Basics. *Concepts Magn Reson Part A*. 2016;45A:e21414. https://doi.org/10.1002/cmr.a.21414

APPENDIX A

PROOF REGARDING COMPOSITE PULSE

In the following, we present the proof that the $90_y270_x90_y$ composite pulse is equivalent to a 180_{-45} pulse:

$$\begin{aligned} R_y\left(\frac{\pi}{2}\right)R_x\left(\frac{3\pi}{2}\right)R_y\left(\frac{\pi}{2}\right) &= R_y\left(\frac{\pi}{2}\right)\underline{R_x\left(\frac{\pi}{4}\right)R_x(\pi)R_x\left(\frac{\pi}{4}\right)}R_y\left(\frac{\pi}{2}\right) \\ &= R_y\left(\frac{\pi}{2}\right)R_x\left(\frac{\pi}{4}\right)R_x(\pi)\underline{R_y\left(\frac{\pi}{2}\right)R_y\left(-\frac{\pi}{2}\right)}R_x\left(\frac{\pi}{4}\right)R_y\left(\frac{\pi}{2}\right) \\ &= R_y\left(\frac{\pi}{2}\right)R_x\left(\frac{\pi}{4}\right)R_x(\pi)R_y\left(\frac{\pi}{2}\right)\underline{R_x(-\pi)R_x(\pi)}R_y\left(-\frac{\pi}{2}\right)R_x\left(\frac{\pi}{4}\right)R_y\left(\frac{\pi}{2}\right) \\ &= \underline{R_y\left(\frac{\pi}{2}\right)R_x\left(\frac{\pi}{4}\right)R_y\left(-\frac{\pi}{2}\right)}R_x(\pi)\underline{R_y\left(-\frac{\pi}{2}\right)R_x\left(\frac{\pi}{4}\right)R_y\left(\frac{\pi}{2}\right)} \\ &= R_z\left(-\frac{\pi}{4}\right)R_x(\pi)R_z\left(\frac{\pi}{4}\right). \end{aligned} \tag{101}$$